OAK RIDGE NATIONAL LABORATORY LIBRARIES
3 4456 0571638 4

ORNL-5604

ornl

OAK
RIDGE
NATIONAL
LABORATORY

UNION
CARBIDE

Materials Heat-to-Heat Variability Study: Part I—Compilation and Analysis of Data

W. J. McAfee W. K. Sartory

This document does not contain UCNI, ECI, or other unclassified sensitive information and has been approved for release to the public by:

David R. Hamrin 11/10/2010
David R. Hamrin, ORNL Classification Officer Date

OAK RIDGE NATIONAL LABORATORY
CENTRAL RESEARCH LIBRARY
CIRCULATION SECTION
4500N ROOM 175
LIBRARY LOAN COPY
DO NOT TRANSFER TO ANOTHER PERSON
If you wish someone else to see this report, send in name with report and the library will arrange a loan.
UCN-7969 3 9-77

[redacted]

OPERATED BY
UNION CARBIDE CORPORATION
FOR THE UNITED STATES
DEPARTMENT OF ENERGY

Printed in the United States of America. Available from
the Department of Energy
Technical Information Center
P.O. Box 62, Oak Ridge, Tennessee 37830

This report was prepared as an account of work sponsored by an agency of the United States Government. Neither the United States Government nor any agency thereof, nor any of their employees, makes any warranty, express or implied, or assumes any legal liability or responsibility for the accuracy, completeness, or usefulness of any information, apparatus, product, or process disclosed, or represents that its use would not infringe privately owned rights. Reference herein to any specific commercial product, process, or service by trade name, trademark, manufacturer, or otherwise, does not necessarily constitute or imply its endorsement, recommendation, or favoring by the United States Government or any agency thereof. The views and opinions of authors expressed herein do not necessarily state or reflect those of the United States Government or any agency thereof.

ORNL-5604
Dist. Category UC-79,
-79h, -79k

Contract No. W-7405-eng-26

Engineering Technology Division

MATERIALS HEAT-TO-HEAT VARIABILITY STUDY: PART I—COMPILATION AND ANALYSIS OF DATA

W. J. McAfee W. K. Sartory

Date Published - November 1980

Prepared by the
OAK RIDGE NATIONAL LABORATORY
Oak Ridge, Tennessee 37830
operated by
UNION CARBIDE CORPORATION
for the
DEPARTMENT OF ENERGY

Contents

Page

ABSTRACT 1

1. INTRODUCTION 1

2. DATA COMPILATION AND ANALYSIS 3
   2.1 Compilation and Criteria Selection 3
   2.2 Evaluation of Prototypical Character of Heats 4
   2.3 Methods of Data Analysis 10

3. RESULTS OF COMPILATION AND ANALYSIS 12
   3.1 Tensile Properties 12
      3.1.1 Tensile yield (0.2%) and ultimate strength 12
      3.1.2 Bilinear yield stress 17
      3.1.3 Cyclic properties and tenth-cycle yield 19
      3.1.4 Plastic modulus and hardening coefficient 21
   3.2 Creep Properties 22
      3.2.1 Stress-rupture properties 22
      3.2.2 Creep deformation 25
   3.3 Fatigue Properties 38
   3.4 Discussion of Cross Correlations 38

4. SUMMARY AND CONCLUSIONS 44

REFERENCES 45

ACKNOWLEDGMENT 47

MATERIALS HEAT-TO-HEAT VARIABILITY STUDY: PART I—COMPILATION AND ANALYSIS OF DATA*

W. J. McAfee W. K. Sartory

ABSTRACT

Heat-to-heat variability of mechanical properties normally used in inelastic analyses was investigated using data from 20 heats of type 304 stainless steel. The results were for use in a sensitivity study to establish the effect of heat-to-heat materials properties variability on the ratchetting strain, creep and fatigue damage, and cyclic life of a long, type 304 stainless steel pipe subjected to ratchetting loading conditions. Criteria and limits on data requirements were established by considering the histogram for the proposed analysis, the structure and material type, and the desirability for an overall consistent data set. Only deformation and failure properties were analyzed. Heat-to-heat variability in properties was found to be statistically significant in three properties: initial bilinear yield, time to rupture, and creep deformation. For other properties considered, either no significant heat variability was evident, or the data sets were too small to provide reliable information.

Keywords: Heat-to-heat variability, type 304 stainless steel, high temperature structural design, inelastic analysis, bilinear yield, creep rupture, fatigue, creep deformation.

1. INTRODUCTION

To assure high performance reliability of elevated temperature nuclear reactor structures, the Department of Energy (DOE) sponsors national programs for the development of advanced design technology. One such program is the High-Temperature Structural Design (HTSD) Program at the Oak Ridge National Laboratory (ORNL), which has as its objective the development of verified high-temperature structural design methods and criteria. In support of program objectives, a study was implemented to determine the sensitivity of current high-temperature design methods to heat-to-heat variations in materials properties and to use this information in assessing the degree of conservatism built into currently recommended design rules.

Materials properties that are used in performing inelastic analyses and in assessing design margins, such as those contained in the *Nuclear Systems Materials Handbook*[1] (NSMH) and the *American Society of Mechanical Engineers Code Case N-47* (Ref. 2) (CCN47), normally represent the composite of many tests on many different heats of material. There are exceptions, particularly in properties for inelastic analysis contained in Ref. 1, where some properties correlations are based on a relatively limited number of heats of material. The variation in properties of a particular heat from the properties values used in evaluating a design will affect the design margins desired. Thus, when the component is fabricated, the designer will not know the degree of conservatism present due to these property variations.

This study was initiated to provide insight into potential effects of material variability on conservatism in design margins. The effort consisted of two phases: (1) compilation of applicable

*Work performed under DOE/RRT AF 15 10 15, Task No. OR-1.1, High-Temperature Structural Design Technology.

material properties data and analysis of heat-to-heat variability of the material properties and (2) use of the data in an inelastic ratchetting analysis of an infinite pipe to study the sensitivity to property variations and to compare the results with current design limits. This report presents the results of the data compilation and analysis effort. A companion report presents results for the sensitivity study.[3]

The inelastic analysis to be performed required properties for type 304 stainless steel—elastic-plastic properties over the temperature range 427 to 593° C (800 to 1100° F), fatigue properties over the temperature range 427 to 593° C (800 to 1100° F), and creep properties at 593° C (1100° F). Deformation and failure data were compiled on 20 heats of material. Using standard statistical methods and employing, wherever possible, accepted mathematical formulations for material properties, heat-dependent correlations were investigated for each property. In some cases, not enough data of the required type were available to permit derivation of heat-dependent correlations. In other cases, strong heat dependency was not apparent. The final results (those used in the subsequent inelastic analyses), indicated heat variability in initial bilinear yield, creep deformation, and creep rupture.

The remainder of this report presents details of the data compilation and analysis. Section 2 deals with data selection and modeling. Section 3 presents results for all properties considered. Finally Sect. 4 provides a summary and recommendations for future work.

2. DATA COMPILATION AND ANALYSIS

2.1 Compilation and Criteria Selection

Using current state-of-the-art methods, ten material properties are required in a general inelastic structural analysis. The first five, the most influential and important, are associated with inelastic deformation and failure and were given primary consideration in collecting and evaluating data. All ten are listed as follows:

1. bilinearized yield stress, (a) monotonic, $\kappa_0(T)$, (b) tenth cycle, $\kappa_1(T)$;
2. slope of plastic portion of stress-strain curve, $E^p(T)$;
3. creep strain vs time at constant stress and temperature, $\epsilon^c(\sigma, t, T)$;
4. time to rupture, $t_r(\sigma, T)$;
5. fatigue strain range, $\epsilon_t(T, N_f)$;
6. Young's modulus, $E(T)$;
7. Poisson's ratio, $\upsilon(T)$;
8. instantaneous thermal expansion coefficient, $\alpha(T)$;
9. volumetric heat capacity, $\rho C_p(T)$;
10. thermal conductivity, $k(T)$.

In the above, T is temperature and N_f is cycles to failure. The general lack of heat-to-heat data led to fixing the last five properties as being heat independent. Values contained in the NSMH[1] were used in the inelastic analyses.

The number of degrees of freedom, with respect to heat variability, in the proposed inelastic analyses was proportional to 4^n where n was the number of random variables (i.e., the number of inelastic analyses required was 4^n with n being the number of independent heat-dependent properties). Thus, there was strong motivation to investigate cross correlations between properties which would, in effect, reduce the value of n.

With this in mind, two criteria were established for selection of data to provide the most consistent overall data set with the greatest probability for developing cross correlations between properties: (1) only material in the laboratory-annealed condition was considered and (2) if possible, only heats were used where two or more of the required properties were available. The assumption was made that the first criterion would lead to greater consistency between properties than use of as-received data. Also, observation revealed that a larger data set for all properties needed was available for the laboratory-annealed compared to as-received material. The second criterion was intended to increase the strength of connection or cross correlation between properties.

Further criteria for data selection were established by consideration of the specific structure and histogram to be analyzed (Fig. 1). This is a type 304 stainless steel pipe rachetting problem involving a plastic cycle followed by a period of isothermal creep. Previous analyses of this problem indicated that the plastic strain range would be ~0.4%. Thus, cyclic stress-strain data for this specific strain range were given primary consideration. The isothermal hold, which also is the maximum temperature in the cycle, is at 593°C (1100°F), and the minimum temperature in the transient is 427°C (800°F). The range of temperature for which elastic-plastic properties were required was established as 400 to 650°C (752 to 1202°F); creep properties were only required at 593°C.

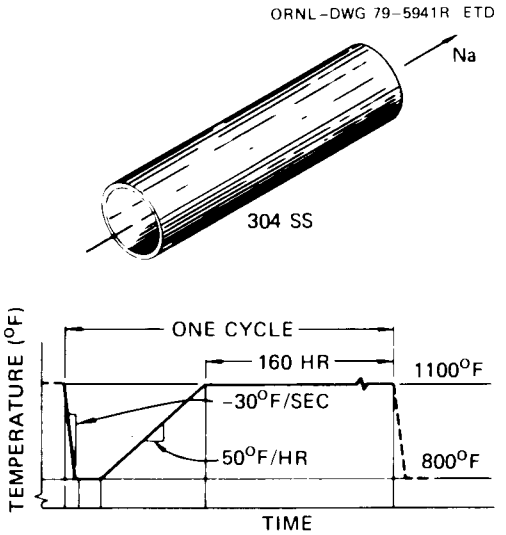

Fig. 1. Structure geometry and load histogram used in inelastic analyses for sensitivity study [°C = 5/9(°F — 32)].

Table 1. Summary of final data set size used in sensitivity study

Property	Size of data subset [heats (points)]
0.2% yield stress	20 (129)
Ultimate strength	20 (118)
Bilinear yield stress	12 (25)
Plastic modulus	12 (25)
Time-to-rupture	19 (229)
Minimum creep rate	19 (232)
Cycles to failure	7 (275)

An extensive amount of data were available on type 304 stainless steel from a study at ORNL of the heat-to-heat variability of mechanical properties. Data were also available from other national and commercial laboratories. Using the selection criteria discussed above, data on 20 heats of type 304 stainless steel were compiled. The extent of the final data set is shown in Table 1.

2.2 Evaluation of Prototypical Character of Heats

For results of the sensitivity study to be valid, some assurance should be provided that the 20 heats selected are reasonably representative of what might be used in actual construction. Two primary specifications required for qualification of type 304 stainless steel for nuclear construction are chemical composition and room temperature mechanical properties. All of the heats were purchased to American Society for Testing and Materials (ASTM) specifications. A thorough discussion of the different product forms and chemical compositions for these heats is contained in Refs. 4 and 5. Table 2, from Ref. 4, shows the vendor, heat number,* and chemical composition of all 20 heats. Heat 11 has a sulfur content of 0.037 wt % compared to a maximum allowable 0.030 wt %. Also, heat 16 has a carbon content of 0.029 wt %, putting it in the type 304L category which allows 0.030 wt % maximum. These two heats were retained in the study because of the amount of data available for them and because they were within specifications in all other respects.

Addressing the room-temperature tensile properties of the materials in the as-received condition, there was a total of 47 yield data points, 45 ultimate strength data points, and 38 uniform elongation data points for these 20 heats. Design according to ASME Section III, Subsection NB (Ref. 6) requires minimum room-temperature properties of yield strength—207 MPa (30 ksi), ultimate strength—517 MPa (75 ksi), and uniform elongation—40%. The distribution, average value, and scatter for the data from each heat were compared with the corresponding ASME minimum property in Figs. 2, 3, and 4. Note that for a number of heats only a single room-temperature data point was available for each property. The single data point was taken as representing the mean for that heat.

*Statement of heat numbers in this report will refer to those assigned for this study, as shown in Table 2.

Table 2. Chemical analyses of type 304 stainless steel—ORNL data

Vendor[a]	Heat No.		Content of element (%)																				
	ID[b]	Actual	C	N	P	B	O	H	Ni	Mn	Cr	Si	Mo	S	Nb	V	Ti	Ta	W	Cu	Co	Pb	Sn
Allegheny	3	337187	0.068	0.031	0.018		0.0042	0.0005	9.43	0.83	18.2	0.59	0.07	0.008	0.0020	0.060	0.003	<0.0005	0.015	0.15	0.05	0.01	0.02
Ludlum	11	55697	0.057	0.034	0.016		0.0150	0.0005	9.38	0.91	18.5	0.50	0.05	0.037	0.0030	0.030	0.002	<0.0005	0.011	0.10	0.05	0.01	0.02
	19	345866	0.044	0.022	0.023	0.0002	0.0096	0.0010	8.98	1.51	18.5	0.47	0.2	0.007	0.0010	0.018	0.0005	0.0005	0.007	0.13	0.04	0.01	0.01
	9	346544	0.063	0.019	0.023	0.0002	0.0081	0.0006	9.12	0.99	18.4	0.47	0.2	0.006	0.0050	0.025	0.017	0.0006	0.026	0.12	0.05	0.01	0.01
	5	337330	0.068	0.031	0.018		0.0042	0.0005	9.43	0.83	18.2	0.59	0.07	0.008	0.0100	0.025	0.002	<0.0005	0.0060	0.15	0.05	0.01	0.02
	18	346845	0.057	0.024	0.023	0.0002	0.0092	0.0013	9.28	0.92	18.4	0.53	0.10	0.006	0.0100	0.050	0.008	<0.0005	0.007	0.11	0.07	0.01	0.01
	13	346779	0.065	0.023	0.024	0.0002	0.0056	0.0009	9.46	0.94	18.1	0.47	0.20	0.005	0.0035	0.029	0.010	0.0020	0.043	0.16	0.02	0.01	0.01
Cameron	2	3121	0.065	0.140	0.019	0.00005	0.0026	0.0011	9.19	1.92	18.1	0.30	0.14	0.010	0.0010	0.035	0.016	<0.0005	0.015	0.07	0.07	<0.0003	0.002
Carlson	7	310390	0.066	0.086	0.018	0.0020	0.0052	<0.0001	8.75	1.57	18.6	0.60	0.30	0.006	0.0160	0.020	0.001	0.0006	0.043	0.20	0.07	0.0007	0.002
	8	600414	0.073	0.058	0.016		0.0190	0.0004	9.52	0.94	18.7	0.69	0.10	0.015	0.0100	0.025	0.002	<0.0005	0.027	0.10	0.05	0.01	0.02
	10	60551	0.043	0.027	0.022	0.0010	0.0220	0.0013	9.40	1.20	18.5	0.59	0.30	0.018	0.0140	0.050	0.025	<0.0005	0.049	0.25	0.08	0.01	0.01
	12	616737	0.064	0.075	0.026	0.00005	0.0072	<0.0001	9.01	1.71	18.3	0.50	0.30	0.012	0.0140	0.031	0.001	<0.0005	0.016	0.50	0.07	<0.0003	0.0050
	6	300380	0.063	0.068	0.018		0.0260	0.0009	8.30	0.97	18.4	0.55	0.07	0.010	0.0100	0.028	0.004	<0.0005	0.016	0.10	0.05	0.01	0.02
	1	544086	0.050	0.043	0.025		0.0091	0.0005	9.46	1.23	18.4	0.53	0.20	0.016	0.0030	0.019	0.006	<0.0005	0.021	0.10	0.05	0.01	0.02
Republic	17	8043813	0.062	0.033	0.044	0.0003			8.95	1.87	17.8	0.48	0.32	0.004	0.0200	0.022	0.002	<0.0005	0.02				
U.S. Steel	14	912796	0.047	0.031	0.029		0.0110	0.0006	9.58	1.22	18.5	0.47	0.10	0.012	0.008	0.037	0.003	<0.0005	0.022	0.10	0.05	0.01	0.02
	16	X22807	0.029	0.021	0.024	0.0005	0.010	0.0012	9.67	1.26	18.8	0.50	0.20	0.023	0.0015	0.012	0.002	<0.0005	0.020	0.11	0.03	0.01	0.01
	15	912797	0.059	0.055	0.028	0.0020	0.0075	0.0007	9.78	1.49	18.3	0.60	0.30	0.011	0.0050	0.020	0.005	0.0005	0.050	0.30	0.07	0.002	0.005
	4	R23283	0.043	0.025	0.018	0.0003	0.0140	0.0009	9.12	1.32	18.2	0.45	0.30	0.020	0.0030	0.030	0.0010	<0.0005	0.021	0.14	0.05	0.01	0.01
	20	R22926	0.053	0.041	0.020		0.0084	0.0007	9.79	1.16	19.0	0.68	0.10	0.025	0.0180	0.050	0.0100	0.0010	0.030	0.070	0.05	0.010	0.02

[a]Allegheny Ludlum = Allegheny Ludlum Steel Corp., Pittsburgh, Pennsylvania; Cameron = Cameron Iron Works, Inc., Houston, Texas; Carlson = Carlson Steel Co., Coatesville, Pennsylvania; Republic = Republic Steel Corp., Cleveland, Ohio; U.S. Steel = United States Steel Corp., Pittsburgh, Pennsylvania.

[b]Identification number used for this study.

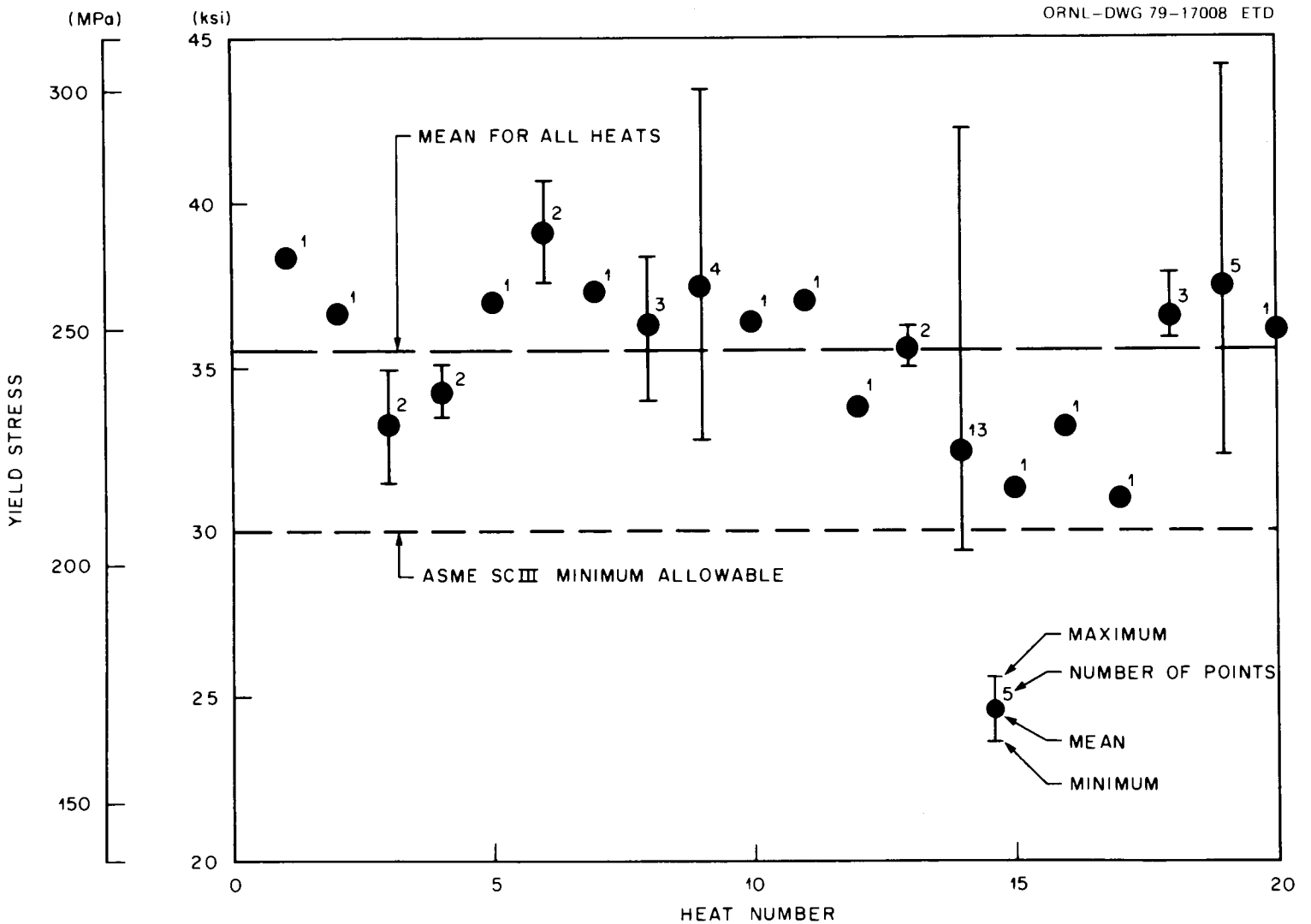

Fig. 2. Heat-to-heat distribution of room temperature yield stress for 20 heats of type 304 stainless steel investigated.

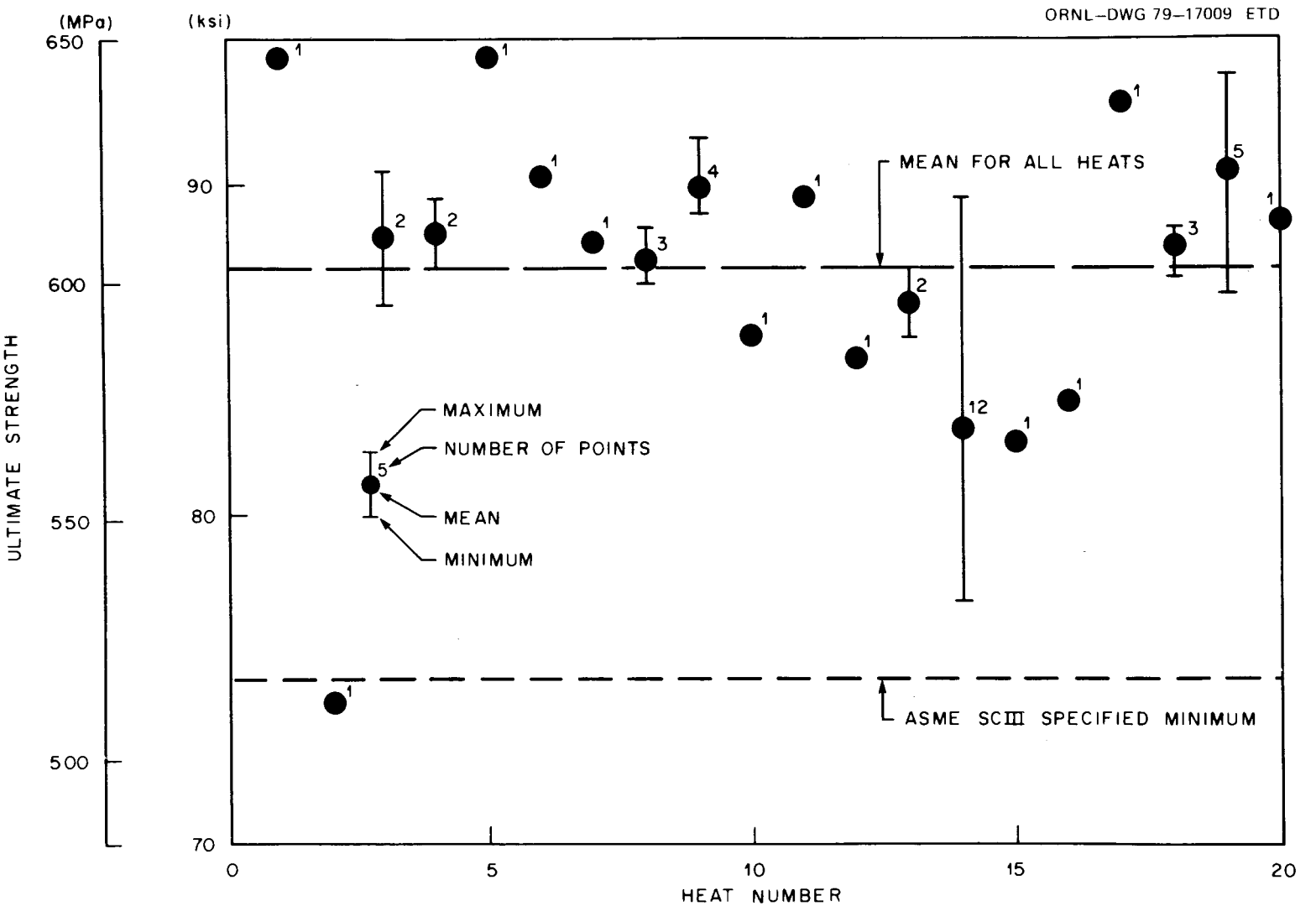

Fig. 3. Heat-to-heat distribution of room temperature ultimate strength for 20 heats of type 304 stainless steel investigated.

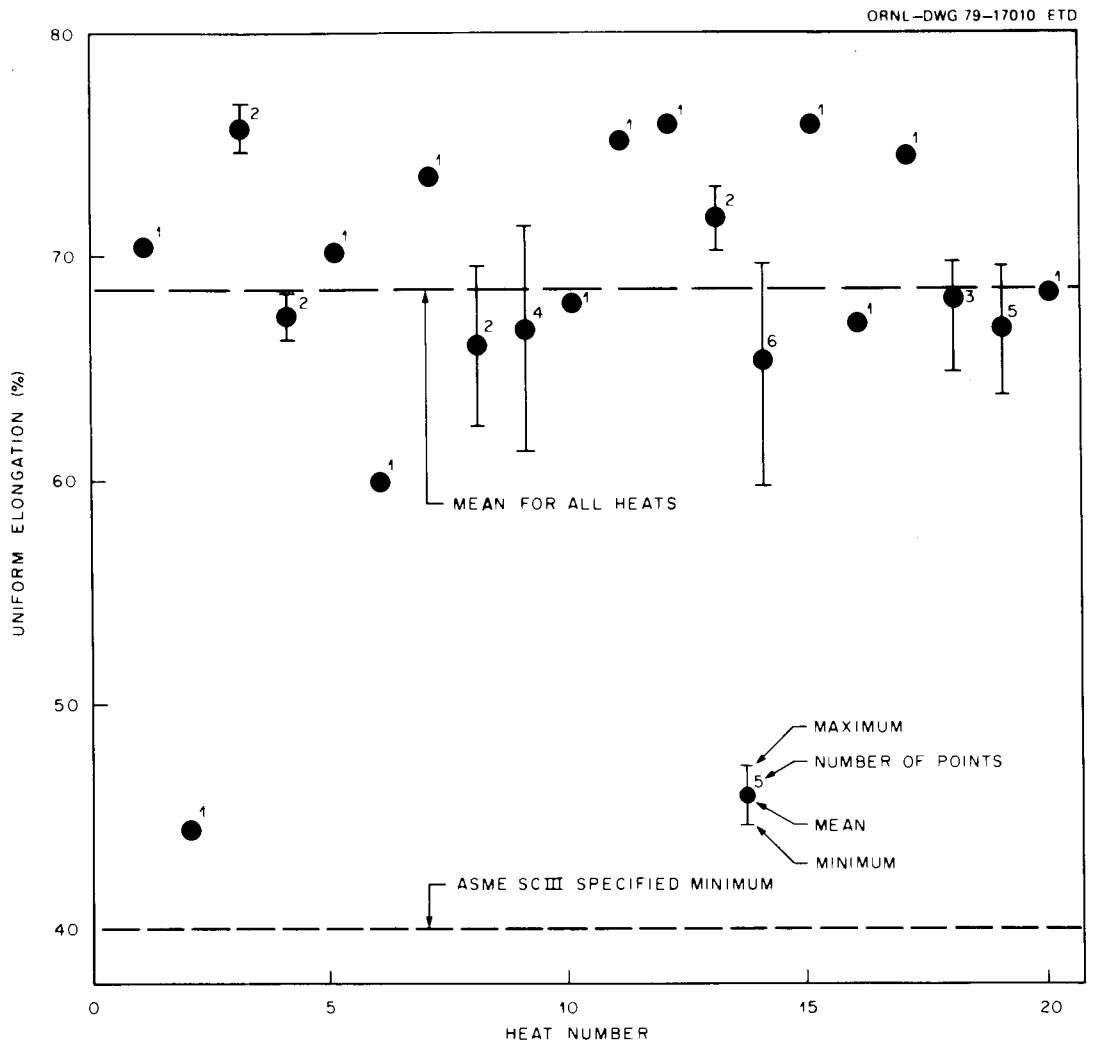

Fig. 4. Heat-to-heat distribution of room temperature uniform elongation for 20 heats of type 304 stainless steel investigated.

For yield strength, only heat 14 has any points below the ASME minimum allowable (Fig. 2). The deviation is due to two points [203 and 205 MPa (29.4 and 29.7 ksi)] of a total of 13 room-temperature tests. For ultimate tensile strength, only heat 2 does not satisfy the ASME limit of 517 MPa (75 ksi) (Fig. 3). Data for this heat consist of a single value, 512 MPa (74.3 ksi). For uniform elongation, all heats satisfy the minimum limit of 40% (Fig. 4). Note that the lowest value of minimum elongation belongs to heat 2, which also had the lowest value of ultimate strength. However, yield strength for this heat approximately equals the mean for all heats.

The heats with chemistry deviations, heats 11 and 16, have properties above the ASME specified limits. More importantly, the behavior of these heats is well within the distribution of data from all heats.

One other comparison was made once the total data set was assembled. Values of as-received yield stress for these heats over the range 400 to 650° C (752 to 1202° F) were compared to the yield stress curve for type 304 stainless steel contained in ASME CCN47 (Ref. 2) (Fig. 5). While the CCN47 curve is

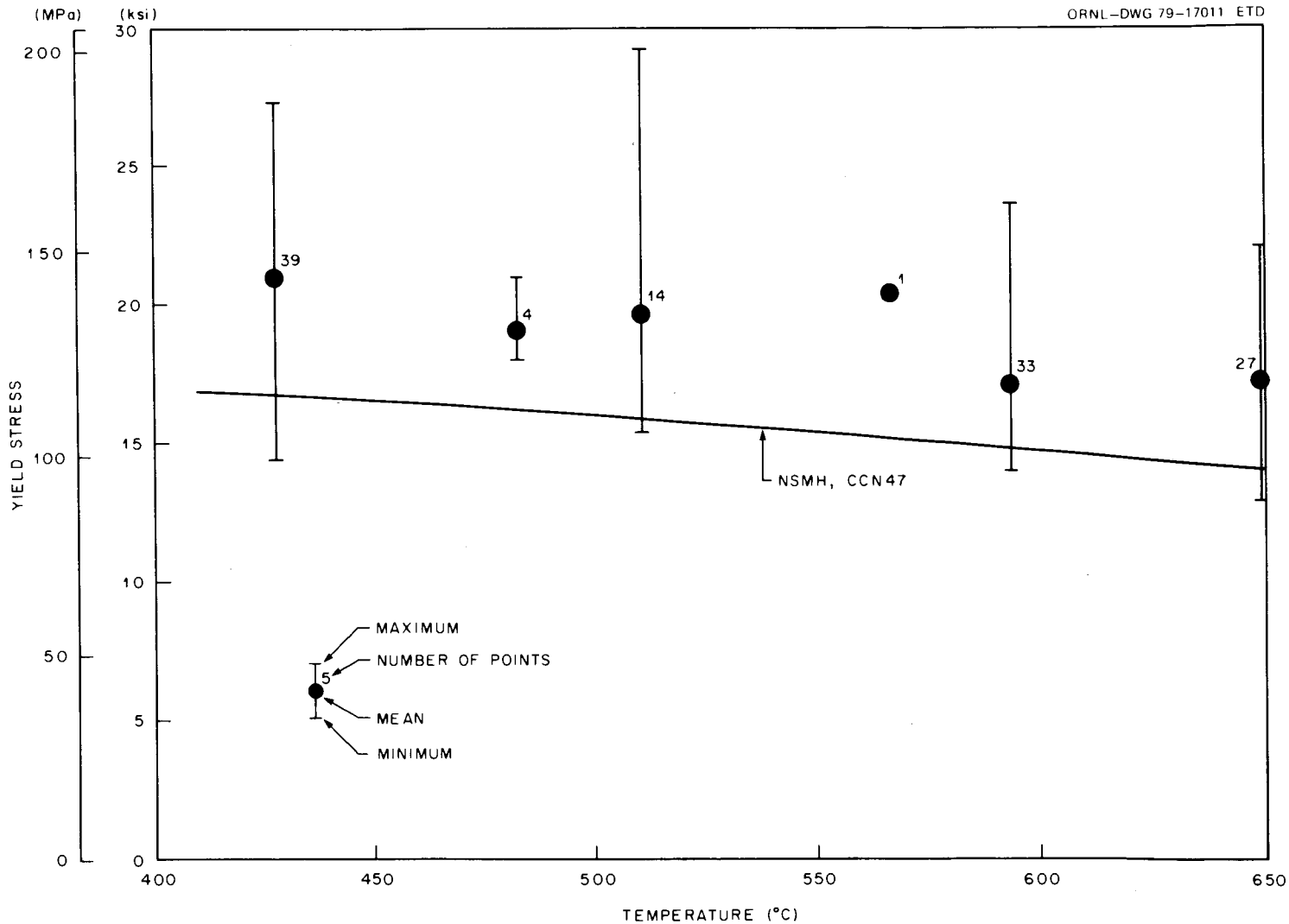

Fig. 5. Comparison of as-received yield strength for 20 heats of type 304 stainless steel with CCN47 values over the range 400–650°C (752–1202°F).

the "best judgement" of the ASME code body (i.e., not specifically related to an average or a minimum value), note that the mean value of as-received yield stress at each temperature is well above the code curve and the lowest or minimum point falls close to the code curve.

While there were minor deviations in chemistry and room-temperature tensile properties from ASTM and ASME specifications, no consistently abnormal heat was observed. The conclusion was made that the heats used are representative of what could be encountered in practice; consequently, the data base for the heat variability study is a valid sampling of type 304 stainless steel behavior.

2.3 Methods of Data Analysis

In compiling and analyzing the data, existing compilations and correlations were used wherever possible with modifications to reflect the particular needs and/or limits of this study. Because the overall study itself was fairly complex, some attention was given to selecting correlation models which were simple to use but would still adequately represent the data.

In this respect, one basic assumption made about the heat behavior of all data was that the heat dependency of a particular property could be represented as a family of parallel curves with heat-dependent intercept values. Mathematically, this can be stated as

$$(\text{property})_{\text{heat}} = (\text{property mean value})_{\text{all heats}} + D_{\text{heat}} ,$$

where D_{heat} represents the deviation of a particular heat from the mean value for all heats (Fig. 6).

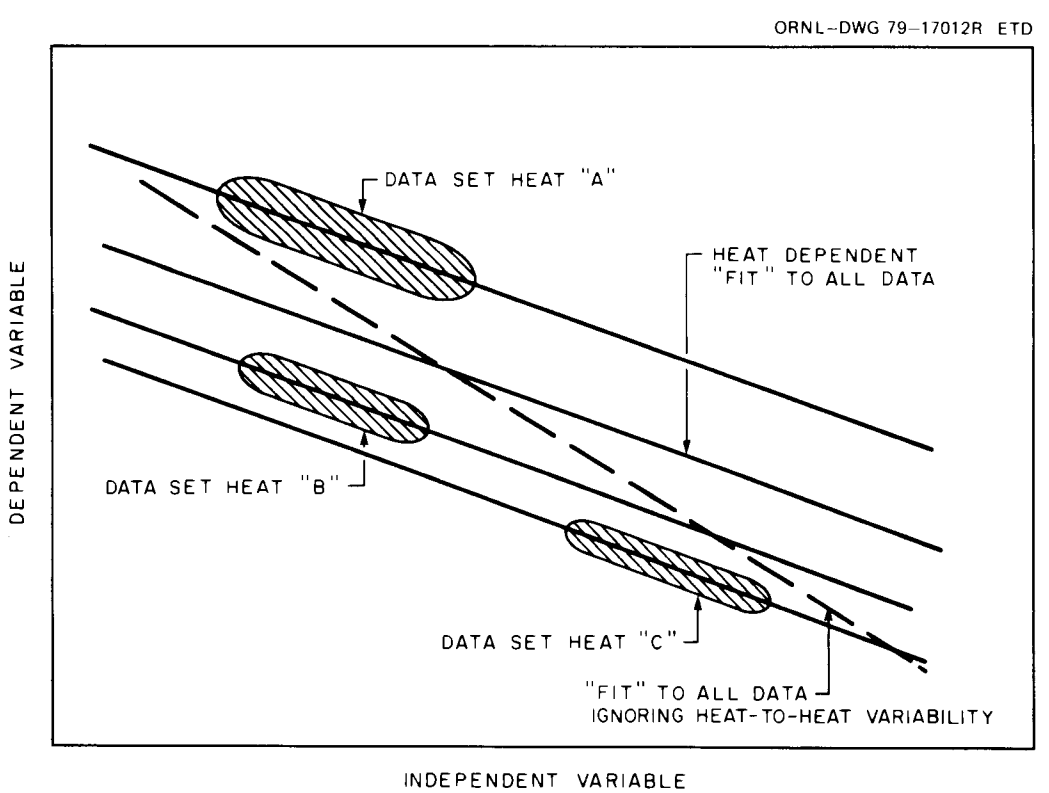

Fig. 6. Schematic representation of family assumption of heat-dependent parallel curves method for treating data.

Treating the data in this manner simplified both data analysis and results usage in the subsequent inelastic analyses.

Several sets of properties were analyzed to investigate the above assumption. The next section illustrates the conclusion that this method of heat-dependent property modeling was adequate for this study.

Data were correlated using least squares-techniques.[7,8] Where the correlation could be represented as a linear function, the method of heat centering was used to obtain the slope. In heat centering, the centroid for each data subset (i.e., the data for each heat) is determined and then all subsets are transported to a common origin. This tends to remove bias caused by the way data are distributed over the data field. For example, referring to Fig. 6, if the data were treated as a single set, the bias caused by distribution of the data subsets would lead to a fit such as that shown by the dashed line. Alternately, centering the data will lead to the heat-dependent fit which more correctly reflects the correlation between independent and dependent variables. With the slope determined, all data points were used to determine the intercept and standard error of estimate for the "average" fit. The intercept value and standard error for each heat was calculated using the common slope and only the data for that heat. These values will be discussed in the next section which presents a treatment of the individual properties.

3. RESULTS OF COMPILATION AND ANALYSIS

3.1 Tensile Properties

3.1.1 Tensile yield (0.2%) and ultimate strength

Tensile properties, though not required as direct input to the inelastic analyses, are used in some property models and are included here for completeness. Tensile data for the 20 heats of type 304 stainless steel used in this study are contained in Refs. 4, 5, and 9 through 12.

For yield strength (0.2%), 129 data points were used to establish a trend curve of yield stress vs temperature over the range 400 to 650° C. Regression analyses indicated the adequacy of an equation of the form*

$$\bar{\sigma}_y = \bar{a}_1 + \bar{a}_2 T \,, \tag{1}$$

where $\bar{\sigma}_y$ is the mean value of yield stress [MPa (ksi)] for all heats, T is temperature (° C), and $\bar{a}_1, \bar{a}_2$ are fitted coefficients. Results of the regression are contained in Table 3. The heat-to-heat variability of yield stress, using the concept discussed in Sect. 2, was modeled by

$$\begin{aligned} \sigma_{y_{\text{heat}}} &= \bar{\sigma}_y + H_{\text{heat}} \\ &= (\bar{a}_1 + H_{\text{heat}}) + \bar{a}_2 T \\ &= a_1 + \bar{a}_2 T \,, \end{aligned}$$

with $\bar{a}_2 = -0.10589$ (-0.01536) for stress in MPa (ksi). Here $\sigma_{y_{\text{heat}}}$ is the yield stress for a particular heat, H_{heat} is a heat dependent adjustment factor from the mean value of yield stress, and a_1 is the heat adjusted value of $\bar{a}_1$. The tabulated results for each heat are contained in Table 4. In addition, a value of standard error of estimate (SEE) is shown for each heat. The fit to all data is shown in Fig. 7. For comparison, reference values[1,2] are shown also. As can be seen, over the specified temperature range, data correlation and reference curves have essentially the same trend, being only slightly displaced from each other.

At this point consider the yield stress correlation as an example to test the assumption of the heat-dependent family of parallel curves concept. To examine this, individual correlations of the Eq. (1)

*Throughout this report, a bar (–) is used to indicate average or mean properties.

Table 3. Summary of results of least-squares fits to tensile yield and ultimate strength data

Property	Order of equation	Least-squares fits [MPa (ksi)]			R^{2a}	SEE[b]
		$\bar{a}_1$	$\bar{a}_2$	$\bar{a}_3$		
Yield stress	1	151.80 (22.01597)	−0.10589 (−0.015358)		0.98284	12.5386 (1.8185)
Ultimate stress	2	117.54 (17.04717)	1.55265 (0.22533)	-1.98123×10^{-3} $(-2.87343 \times 10^{-4})$	0.99686	20.4582 (2.9671)

[a]Correlation coefficient.
[b]Standard error of estimate.

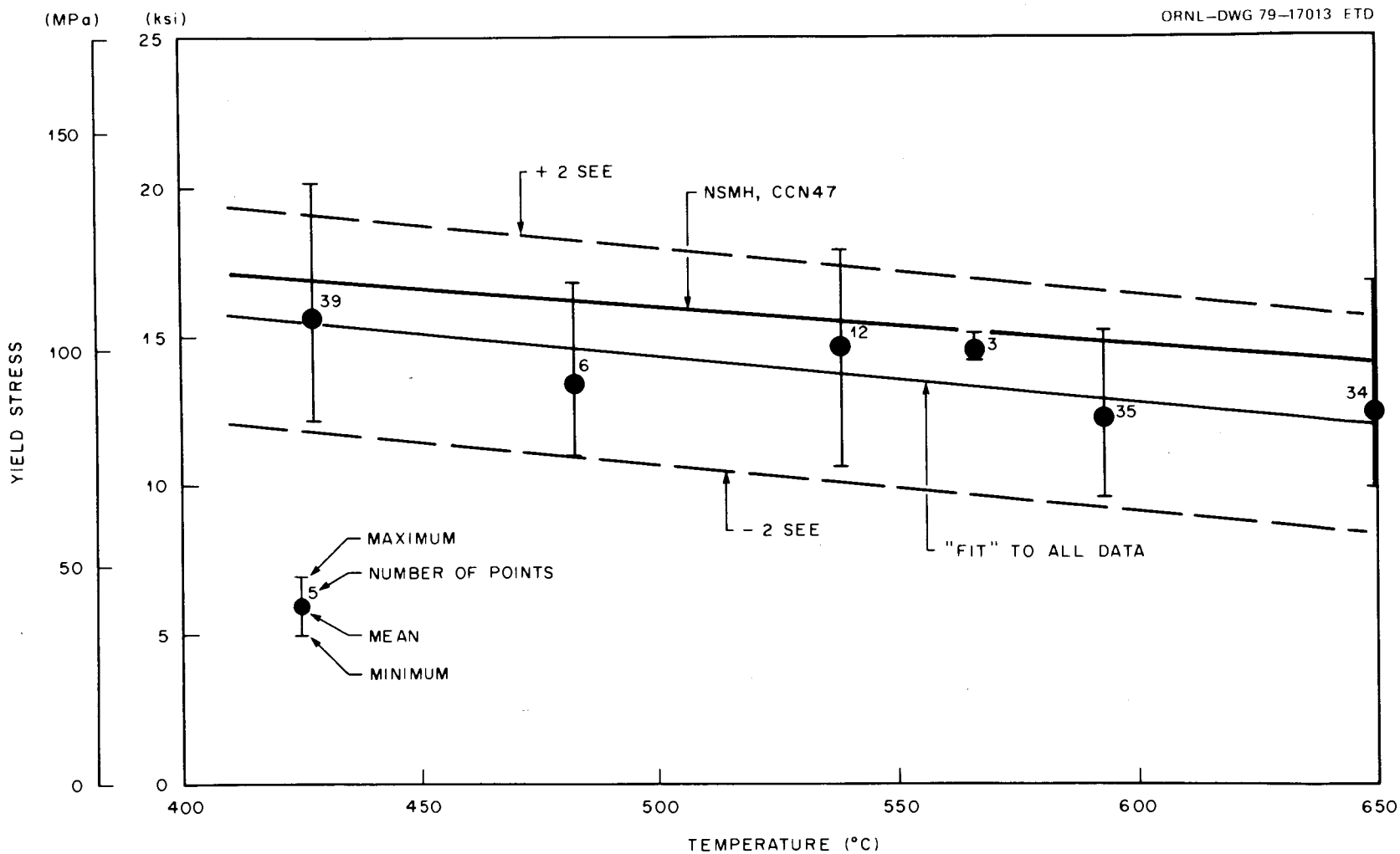

Fig. 7. Yield stress (0.2%) vs temperature for reannealed type 304 stainless steel over the range 400–650°C (752–1202°F).

Table 4. Heat-to-heat variability of yield stress (0.2%) function

Heat identification No.	Points per heat	Yield stress parameters [MPa (ksi)]		
		a_1	H	SEE
1	3	153.1437 (22.2108)	1.3436 (0.1949)	1.5857 (0.2300)
2	3	150.6155 (21.8442)	−1.1846 (−0.1718)	2.2770 (0.3302)
3	3	141.8819 (20.5775)	−9.9182 (−1.4385)	3.1098 (0.4510)
4	3	145.3294 (21.0775)	−6.4707 (−0.9385)	3.0499 (0.4423)
5	3	165.0950 (23.9442)	13.2949 (1.9282)	1.0702 (0.1552)
6	6	165.0037 (23.9309)	13.2036 (1.9150)	2.6849 (0.3894)
7	6	151.6498 (21.9942)	−0.1503 (−0.0218)	1.9036 (0.2761)
8	7	159.3562 (23.1118)	7.5561 (1.0959)	5.5185 (0.8004)
9	3	160.9580 (23.3442)	9.1579 (1.3282)	5.8635 (0.8504)
10	3	155.3284 (22.5277)	3.5283 (0.5117)	8.7367 (1.2671)
11	25	161.5360 (23.4280)	9.7359 (1.4120)	12.8020 (1.8567)
12	6	152.3393 (22.0942)	0.5392 (0.0782)	5.3468 (0.7755)
13	3	164.4055 (23.8442)	12.6054 (1.8282)	4.1807 (0.6063)
14	27	136.5599 (19.8056)	−15.2402 (−2.2103)	8.7505 (1.2691)
15	3	139.8134 (20.2775)	−11.9867 (−1.7385)	3.6184 (0.5248)
16	6	148.6443 (21.5583)	−3.1558 (−0.4577)	3.9230 (0.5690)
17	8	150.5094 (21.8288)	−1.2907 (−0.1872)	4.1390 (0.6003)
18	4	157.5341 (22.8476)	5.7340 (0.8316)	9.5790 (1.3893)
19	4	152.8800 (22.1726)	1.0799 (0.1566)	13.2839 (1.9266)
20	3	153.3753 (22.2442)	1.5734 (0.2282)	2.9558 (0.4287)

form were determined for each heat (i.e., the data for each heat were treated as totally independent data sets). A heat-by-heat comparison was made with the resulting value of a_2 and that contained in Table 3. Two cases were of interest: (1) the maximum algebraic deviation of coefficient a_2 for any heat from the value shown in Table 3 and (2) the minimum algebraic deviation of coefficient a_2 for any heat from the value shown in Table 3. The results of this comparison are shown in Table 5, which includes for each heat the individual values of a_1 and a_2 and the percent deviation of a_2 from the average value in Table 3. Heat 13 satisfies case 1 while heat 10 satisfies case 2 (Table 3). In addition, a third case of interest is marked—that for the maximum absolute deviation of coefficient a_1 for any heat from the value shown in Table 3. The results for these cases are shown in Fig. 8. Even though the maximum absolute deviation of the heat dependent a_2 values from $\bar{a}_2$ seem large, the agreement between the individual and adjusted fits is considered acceptable (Fig. 8). The simplification introduced in both data analyses and subsequent inelastic analyses using the family of parallel curves concept seems to be justified when one observes the relatively small error introduced over treating data for each heat as an independent data set.

Ultimate tensile strength data were treated in the same manner as yield stress data. Regression analyses indicated that an adequate description of data over the temperature range 400 to 650° C (750 to 1200° F) is provided by an equation of the form

$$\bar{\sigma}_u = \bar{a}_1 + \bar{a}_2 T + \bar{a}_3 T^2 , \tag{2}$$

where $\bar{\sigma}_u$ is the mean value of ultimate strength [MPa (ksi)] for all data, T is the temperature (° C), and $\bar{a}_1$, $\bar{a}_2$, $\bar{a}_3$ are fitted coefficients. Results of the regression coefficients are shown in Table 3. The comparison of the data and the correlation is shown in Fig. 9. Also, the curve recommended in the NSMH[1] is shown for comparison.

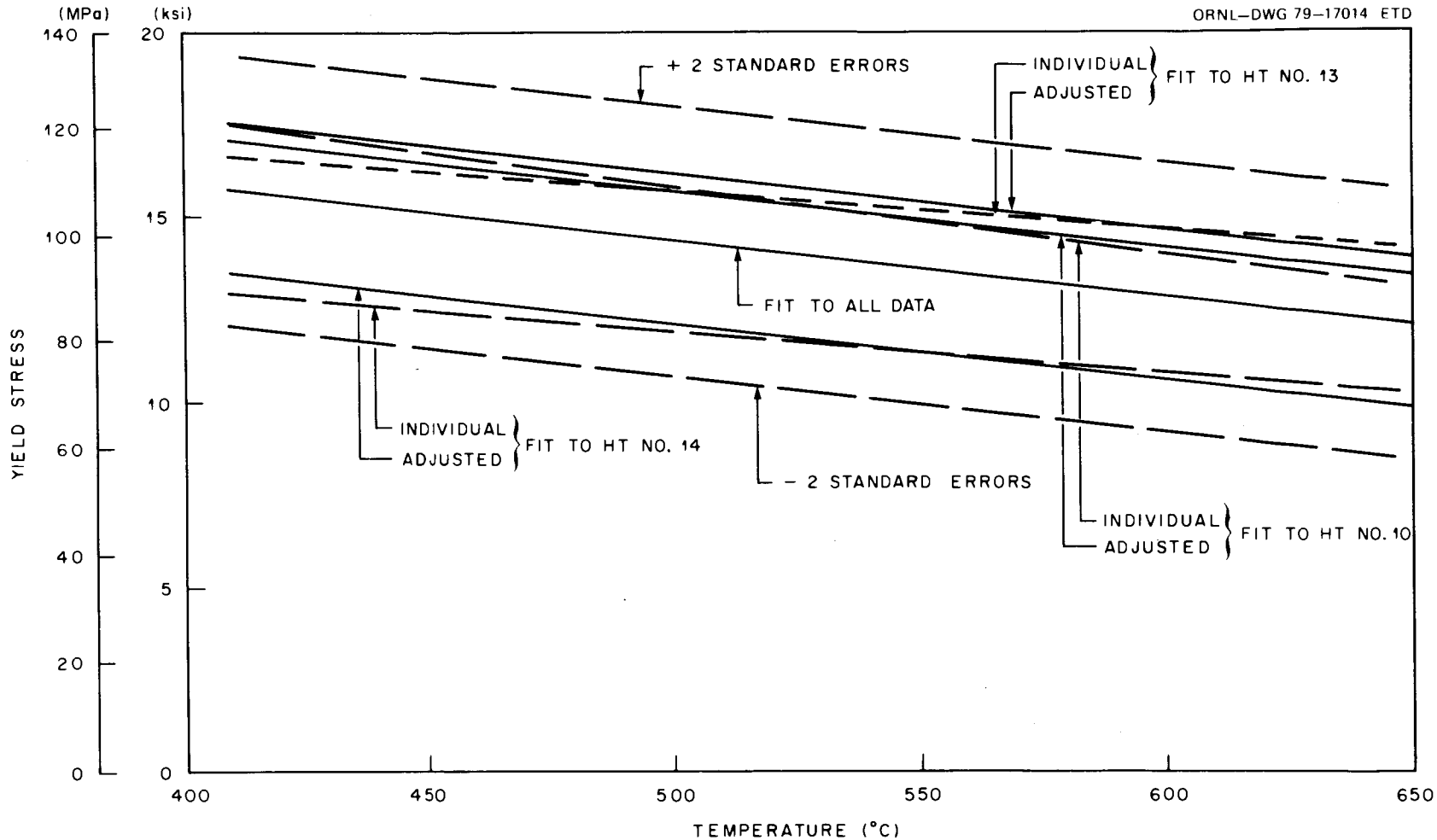

Fig. 8. Comparison of "adjusted" fits to actual fits of yield stress (0.2%) vs temperature for three cases of worst correlation.

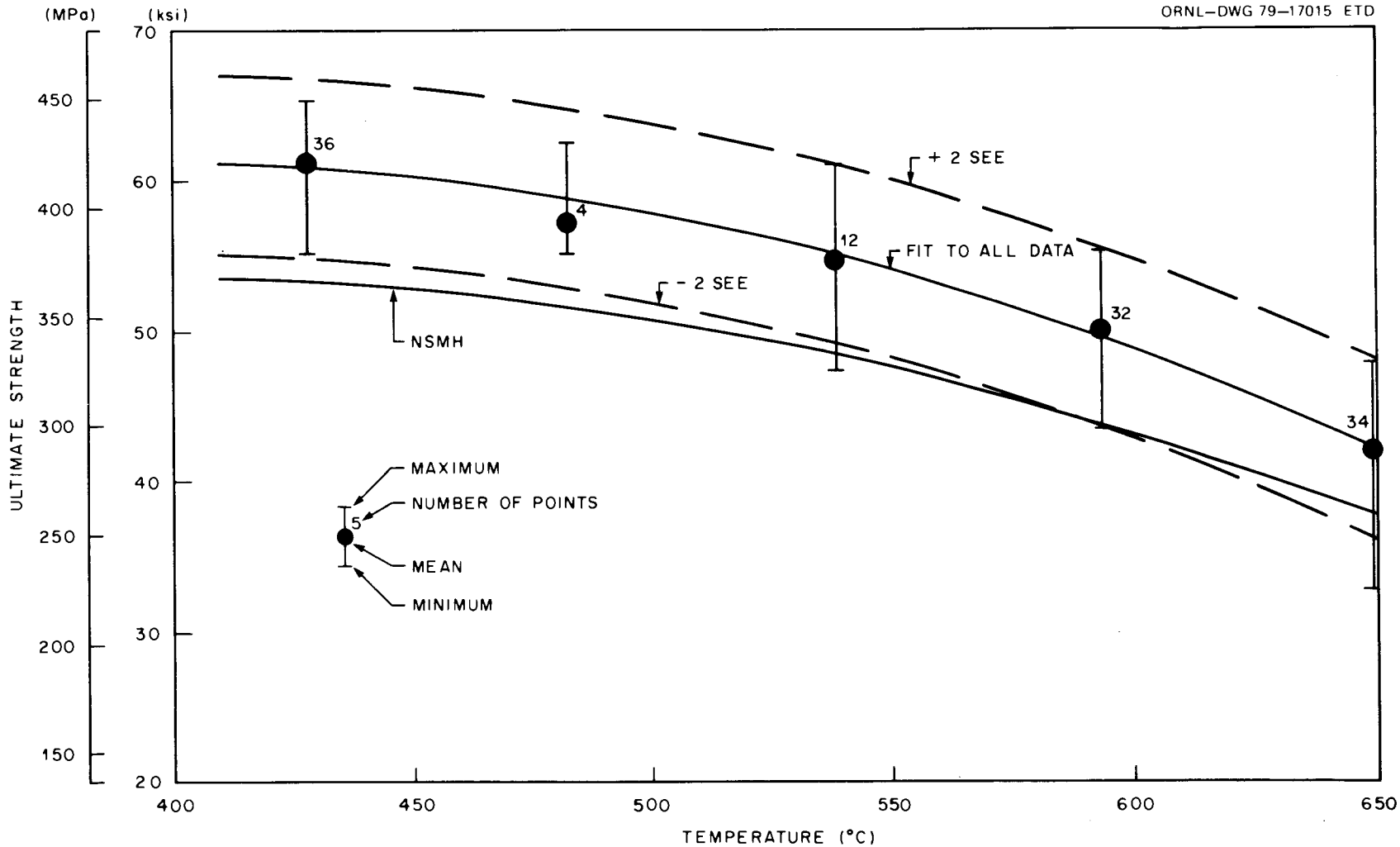

Fig. 9. Ultimate tensile strength vs temperature over the range 400–650° C (752–1202° F) for 20 heats of type 304 stainless steel.

Table 5. Comparison of coefficients a_1 and a_2 obtained from fits to yield stress data for each heat taken individually

Heat No.	Yield stress data (MPa)			Case
	a_1	a_2	Δa_2[a]	
1	146.64	−0.0942	11.0	
2	148.34	−0.1018	3.9	
3	127.14	−0.0794	25.0	
4	138.53	−0.0936	11.6	
5	169.24	−0.1135	−7.0	
6	172.96	−0.1211	−14.3	
7	148.18	−0.0996	5.9	
8	165.01	−0.1162	−9.8	
9	160.23	−0.1046	1.2	
10	172.80	−0.1268	19.7	2
11	164.46	−0.1113	−5.1	
12	137.68	−0.0795	24.9	
13	146.22	−0.0732	30.8	1
14	121.55	−0.0785	25.9	3
15	127.48	−0.0837	20.9	
16	132.69	−0.0772	27.1	
17	147.93	−0.1011	4.5	
18	158.26	−0.1073	−1.3	
19	153.00	−0.1134	−7.1	
20	139.15	−0.0803	24.1	

[a]Deviation of a_2 for each heat from $\bar{a}_2$, Table 3. $\Delta a_2 = (\bar{a}_2 - a_2) \times 100/\bar{a}_2$.

The heat-to-heat variability of $\bar{\sigma}_u$ was modeled by

$$\begin{aligned}\sigma_{u_{heat}} &= \bar{\sigma}_u + F_{heat} \\ &= (\bar{a}_1 + F_{heat}) + \bar{a}_2 T + \bar{a}_3 T^2 \\ &= a_1 + \bar{a}_2 T + \bar{a}_3 T^2 ,\end{aligned}$$

where $\sigma_{u_{heat}}$ is the ultimate stress for a particular heat, F_{heat} is a heat dependent adjustment factor, a_1 is the heat adjusted value of $\bar{a}_1$, and $\bar{a}_2$ and $\bar{a}_3$ are the same as in Eq. (2), Table 3. These results are shown in Table 6.

3.1.2 Bilinear yield stress

Only a limited amount of data is available on the bilinear yield stress and hardening parameters for type 304 stainless steel.[12–15] Furthermore, these data seem to all be for a single heat of material (heat 14). Thus, the recommendation was made that the initial bilinear yield, the tenth cycle yield, and the hardening parameter C be taken as heat independent, and that values from the NSMH[1] be used. Preliminary inelastic structural analyses indicated that the deformation and failure results were very sensitive to the values of yield and the hardening parameters used. Therefore, the conclusion was made that some heat variability of these parameters was required.

In lieu of an adequate data base, the initial bilinearized stress-strain curve was related to conventional stress-strain parameters. Using only data for the ORNL reference heat [HT 9T2796 (heat 14 for this study)], a close relationship was observed between the temperature dependency of 0.2% yield and initial bilinear yield (for a 0.4% strain range) as is shown in Fig. 10. The "adjusted" curve through

Table 6. Heat-to-heat variability of ultimate stress function

Heat identification No.	Ultimate stress parameters [MPa (ksi)]		
	a_1	F	SEE
1	126.3813 (18.3294)	8.8410 (1.2822)	11.6265 (1.6862)
2	87.7693 (12.7294)	−29.7710 (−4.3178)	13.7471 (1.9938)
3	101.7891 (14.7627)	−15.7511 (−2.2844)	13.3380 (1.9344)
4	125.4619 (18.1961)	7.9217 (1.1489)	6.1657 (0.8942)
5	126.6111 (18.3627)	9.0709 (1.3156)	21.7274 (3.1512)
6	133.9658 (19.4294)	16.4255 (2.3822)	13.0019 (1.8857)
7	141.2055 (20.4794)	23.6653 (3.4322)	5.2173 (0.7567)
8	138.0921 (20.0279)	20.5518 (2.9807)	16.3313 (2.3686)
9	130.7481 (18.9627)	13.2079 (1.9156)	13.4628 (1.9525)
10	103.5171 (15.0134)	−14.0231 (−2.0338)	53.6719 (7.7842)
11	112.0467 (16.2504)	−5.4935 (−0.7967)	20.3934 (2.9577)
12	141.2055 (20.4794)	23.6653 (3.4322)	6.6711 (0.9675)
13	129.1393 (18.7294)	11.5990 (1.6822)	12.6466 (1.8342)
14	105.8485 (15.3515)	−11.6917 (−1.6957)	14.2413 (2.0655)
15	122.7039 (17.7961)	5.1637 (0.7489)	0.8324 (0.1207)
16	90.7637 (13.1637)	−26.7765 (−3.8835)	11.7637 (1.7061)
17	134.6820 (19.5333)	17.1417 (2.4861)	15.9452 (2.3126)
18	130.9779 (18.9961)	13.4377 (1.9489)	28.6979 (4.1621)
19	113.5318 (16.4658)	−4.0084 (−0.5813)	15.9250 (2.3096)
20	118.3371 (17.1627)	0.7969 (0.1156)	6.6905 (0.9703)

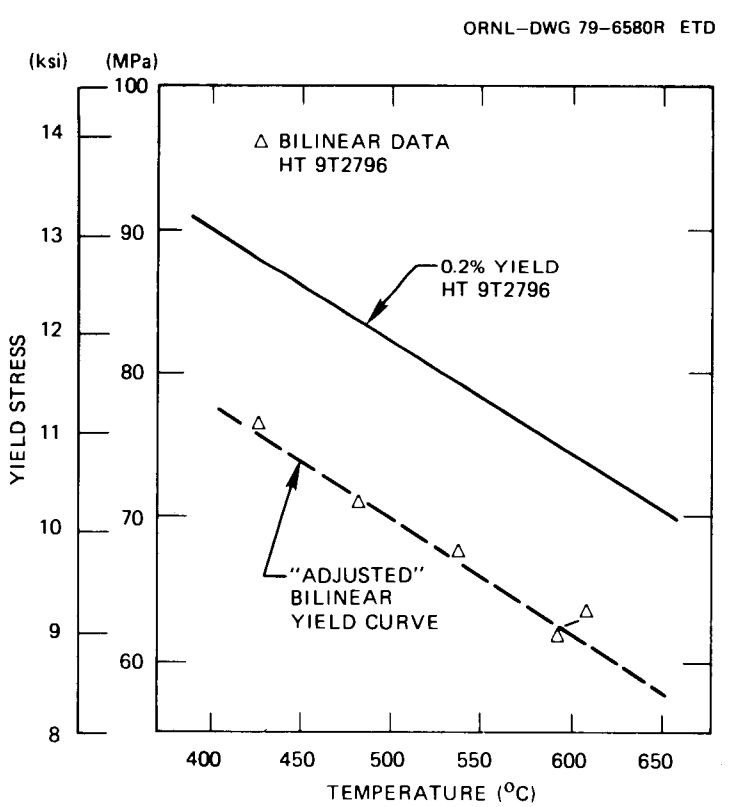

Fig. 10. Yield stress (0.2%) and initial bilinear yield (0.4% strain range) vs temperature over the range 400–650°C (752–1202°F) for a single heat of type 304 stainless steel (1 ksi = 6.895 MPa).

the initial bilinear yield (for a 0.4% strain range) data has the same slope as the 0.2% yield curve, but the intercept was determined in a least-squares sense. As can be seen, a very respectable representation of bilinear yield results is obtained. Thus, the assumption was made that all heats would behave in the same way, that is, the bilinear yield (0.4% strain range) for a particular heat would have the same temperature dependency as the 0.2% yield but would be displaced by some factor.

To determine this factor, initial stress-strain data were obtained on all 20 heats of material.[16] For the curves that could be well defined below 0.2% strain, bilinearization was performed using the procedure in Ref. 17, and values of initial yield σ_{y_0} and plastic slope E^p were measured. Values of the initial yield parameter κ_0 and the hardening coefficient C were calculated. It was determined that the initial bilinear yield could be represented by

$$\bar{\sigma}_{y_0} = \bar{a}_1 + \bar{a}_2 T , \tag{3}$$

where

$\bar{\sigma}_{y_0}$ = average (all heats) initial bilinear yield stress in MPa (ksi),

T = temperature in °C,

$\bar{a}_1$ = 138.78 (20.1273),

$\bar{a}_2$ = −0.10589 (−0.015358),

with a standard error of 8.929 (1.295). The desired adjustment factor was then 138.78/151.80 = 0.914, and the initial bilinear yield for any heat becomes

$$\sigma_{y_0} = 0.914\, a_1 + \bar{a}_2 T , \tag{4}$$

where a_1 is the heat-dependent coefficient on 0.2% yield stress listed in Table 4 and $\bar{a}_2$ is as shown in Eq. (3) and Table 3.

3.1.3 Cyclic properties and tenth-cycle yield

As above, lack of an adequate data base prevented conclusive heat and temperature treatment of cyclic hardening and tenth-cycle yield. A detailed development of these properties, based on an incremental yield increase with plastic strain accumulation $\bar{E}^p$, has been performed for the ORNL reference heat[18] and is shown in Fig. 11. This development is more refined than a jump to tenth cycle and has a more realistic structural behavior.

Thus, the assumption was made that each heat would harden in the same manner, and the data shown in Fig. 11 were normalized to the initial bilinearized yield. The results are shown in Table 7. The mean value of yield stress at the ith step for any temperature and accumulated plastic strain is

$$\bar{\sigma}_{y_i} = \bar{\sigma}_{y_0} + Y(\bar{\epsilon}^p, T) , \tag{5}$$

where the value of $Y(\bar{\epsilon}^p, T)$ is interpolated from Table 7. Obviously the deviation on $\bar{\sigma}_{y_i}$ will be the same as that for $\bar{\sigma}_{y_0}$. For individual heats, the value σ_{y_i} is calculated from Eq. (5) using the heat dependent σ_{y_0} value from Eq (4).

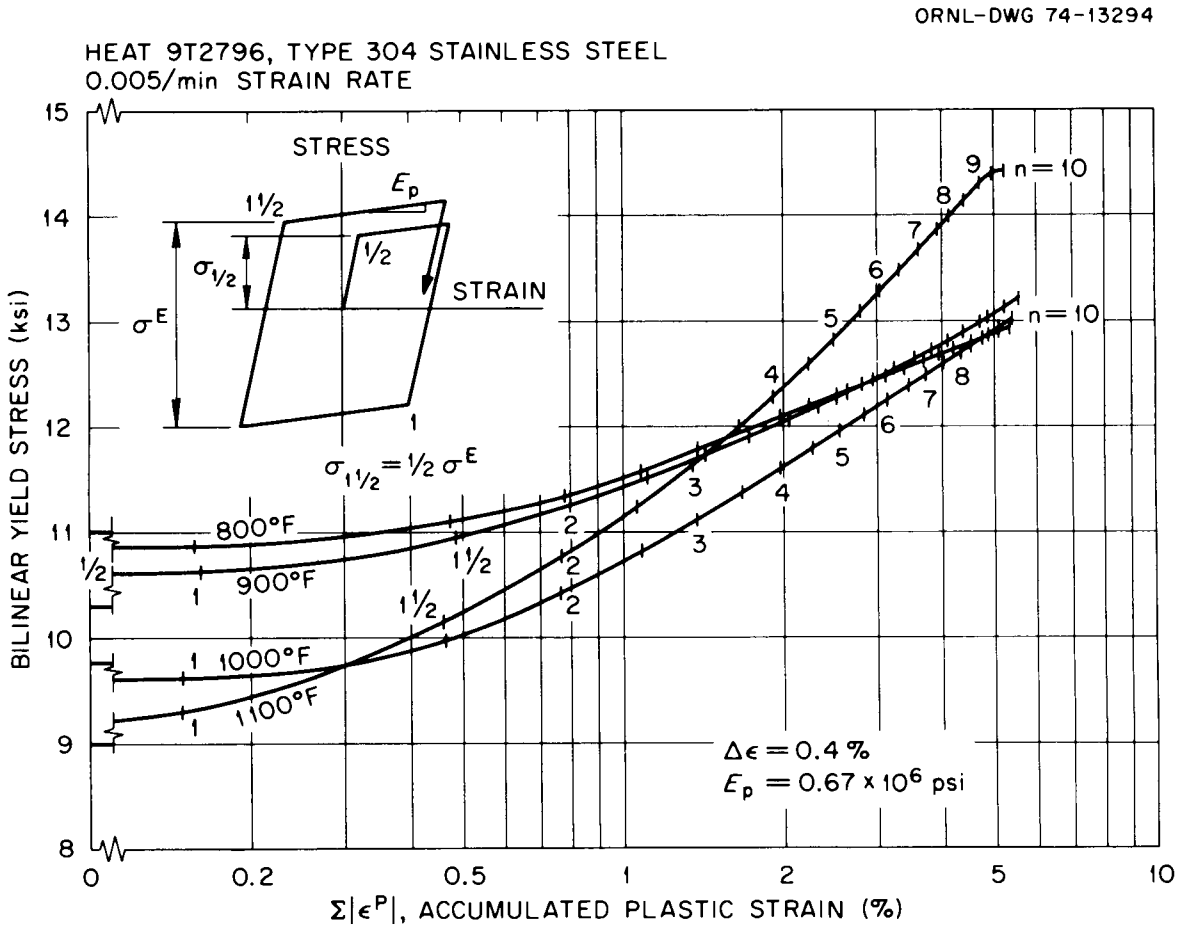

Fig. 11. Dependence of bilinear yield stress on temperature and accumulated plastic strain for ORNL reference heat of type 304 stainless steel.

Table 7. Normalized bilinear yield stress Y vs accumulated plastic strain and temperature

$\bar{\epsilon}^p$ (m/m)	Normalized stress (MPa)[a] at temperature			
	427°C	482°C	538°C	593°C
0.005	0.393	4.840	1.806	8.715
0.01	3.254	8.205	6.481	14.845
0.02	7.054	12.390	12.632	23.071
0.03	9.432	15.176	16.493	29.207
0.04	11.260	17.389	19.361	34.048
0.05	12.687	19.444	21.657	37.350
0.058	13.080	20.513	22.560	37.592
1.0	13.080	20.513	22.560	37.592

[a] σ_y (psi) = 145 σ_y (MPa).

3.1.4 Plastic modulus and hardening coefficient

The mean value of E^p was found to be 6.666 MPa (0.966×10^6 psi). The number of data points available, as with initial bilinear yield, would not permit a conclusive statistical treatment of temperature and heat-dependent plastic modulus. With respect to temperature, referring to the work by Maiya,[12] the particular strain range selected for this study seems to be a threshold between smaller strain ranges that are highly temperature sensitive and larger strain ranges that are essentially insensitive to temperature, Fig. 12. With respect to heat variability, no consistent relationship between plastic modulus and some other tensile property was evident such that a construction comparable to that for initial bilinear yield could not be performed. For the subsequent inelastic analyses, the mean value of E^p at 593° C and the corresponding elastic modulus E from Ref. 1 were used in defining the hardening coefficient C where

$$C = \frac{2}{3} \frac{EE^p}{(E^p - E)} ,$$

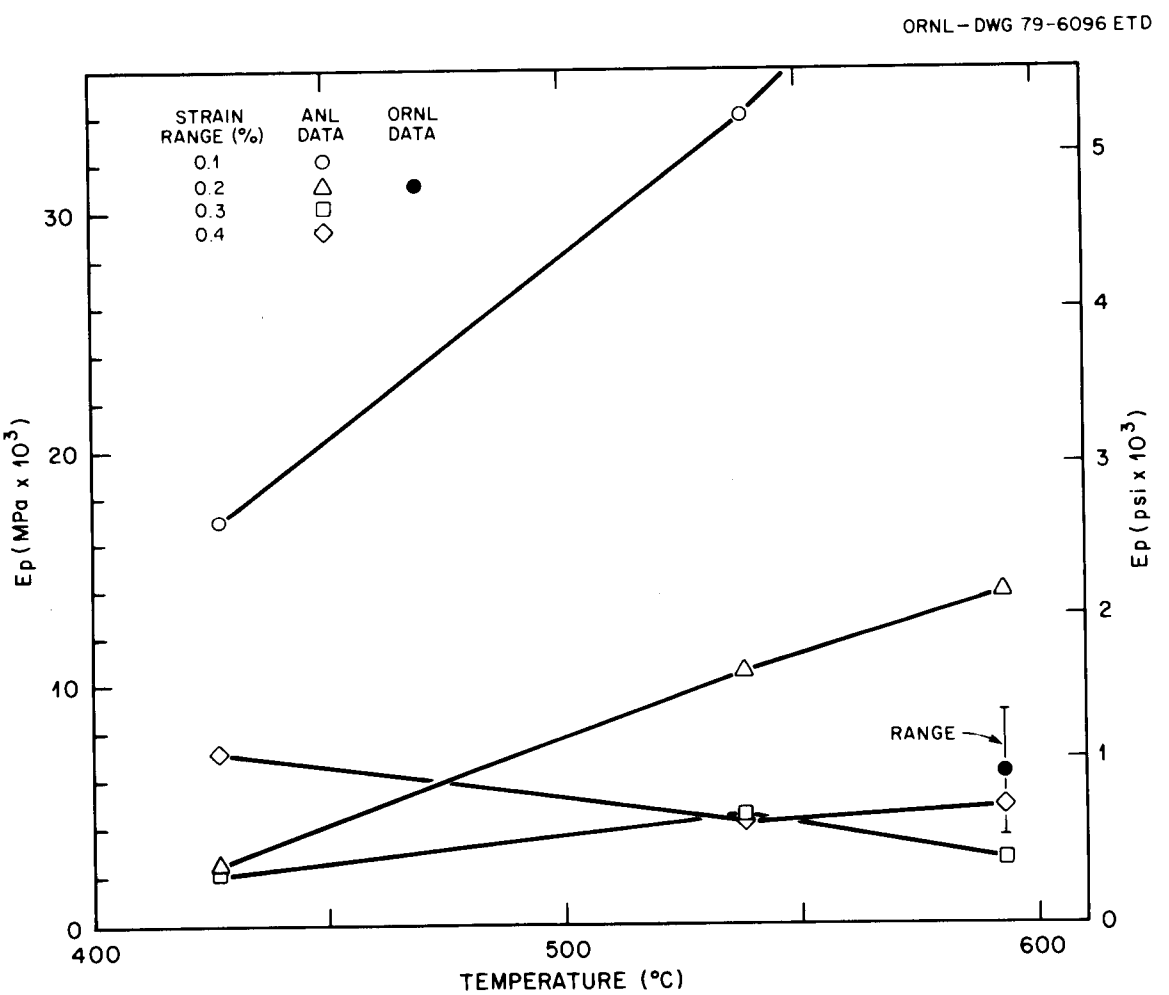

Fig. 12. Temperature and strain range dependence of plastic modules for annealed type 304 stainless steel.

and

$$C = 4651 \text{ MPa } (0.675 \times 10^6 \text{ psi}) ,$$

and that C be taken as heat and temperature independent. Note at this point that the recommended value of E^p is approximately one half the value from the NSMH[1] for a strain range of 0.4%.

3.2 Creep Properties

3.2.1 Stress-rupture properties

Creep deformation and creep-rupture information were needed for the inelastic deformation and failure analyses. As observed in a preliminary assessment of the data, creep deformation, through minimum creep rate $\dot{\bar{\epsilon}}_m$, correlated with time-to-rupture $\bar{t}_r$ (Fig. 13). This correlation implied that the same functional form should be used to describe the stress dependence of $\dot{\bar{\epsilon}}_m$ and $\bar{t}_r$. In addition, the functional form chosen for $\dot{\bar{\epsilon}}_m$ (and thus $\bar{t}_r$) had an important effect on creep deformation. Ultimately, selecting a form for minimum creep rate that provided the best comparison between predicted total creep strain and experimental creep data became necessary. This is discussed in greater detail in Sect. 3.2.2. Only the final results for time-to-rupture are presented here.

The extensive work contained in Refs. 19 and 20 supplemented by additional data from Refs. 4, 9, and 21 through 23 formed the basis for treatment of time-to-rupture. Considering only data at 593° C, 229 data points from 19 heats of material were available to establish a "master" creep-rupture curve. Consideration was given to several functional forms for representing the data. Based on previous work[19,20] in conjunction with the criteria on creep strain discussed above, a power law formulation was used,

$$\bar{t}_r = \bar{a}_1 \sigma^{\bar{a}_2} , \tag{6}$$

where $\bar{t}_r$ is mean time to rupture for all heats, σ is stress (MPa), and $\bar{a}_1$, $\bar{a}_2$ are regression coefficients. Results of the fit to all data are given in Table 8. Data and fit are compared in Fig. 14. Heat-to-heat variability was computed based on the equation

$$\begin{aligned} \log (t_r)_{\text{heat}} &= \log \bar{t}_r + \log B_{\text{heat}} \\ &= \log (\bar{a}_1 B_{\text{heat}}) + \bar{a}_2 \log \sigma \\ &= \log a_1 + \bar{a}_2 \log \sigma . \end{aligned}$$

Variability results are summarized in Table 9.

A comparison of the results in Eq. (6) with CCN47 creep-rupture design curve[2] is shown in Fig. 15. The minimum rupture curve as defined by this study agrees well with the CCN47 curve. This does not necessarily imply that the average curves would agree because different data sets were used to establish each curve and different margins may have been used to define the minimum curve. Note that at the stress and time levels of interest for this study, the agreement between the two minimum curves is almost exact.

ORNL-DWG 79-6095 ETD

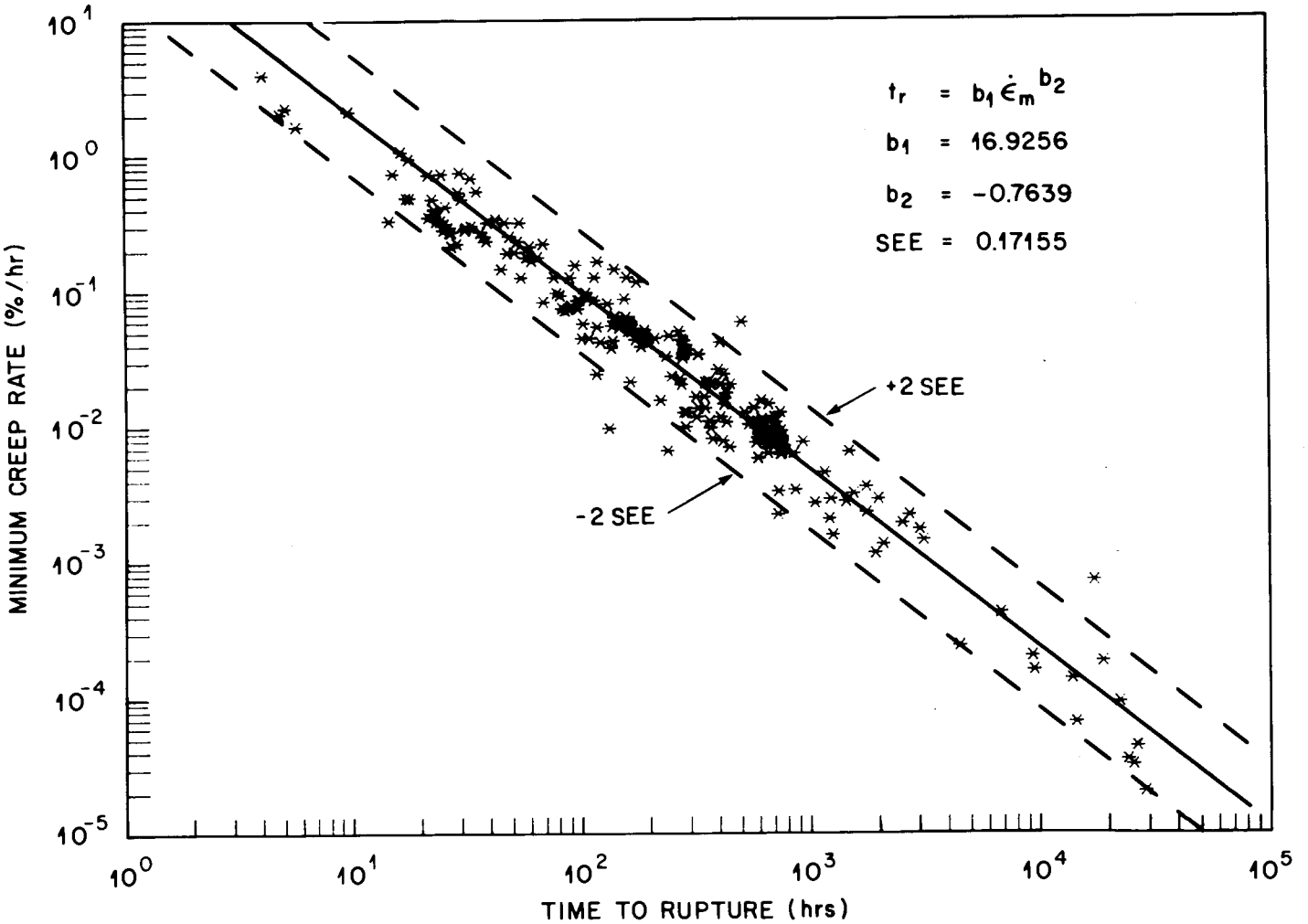

Fig. 13. Correlation between time-to-rupture and minimum creep rate at 593°C (1100°) for 19 heats of annealed type 304 stainless steel.

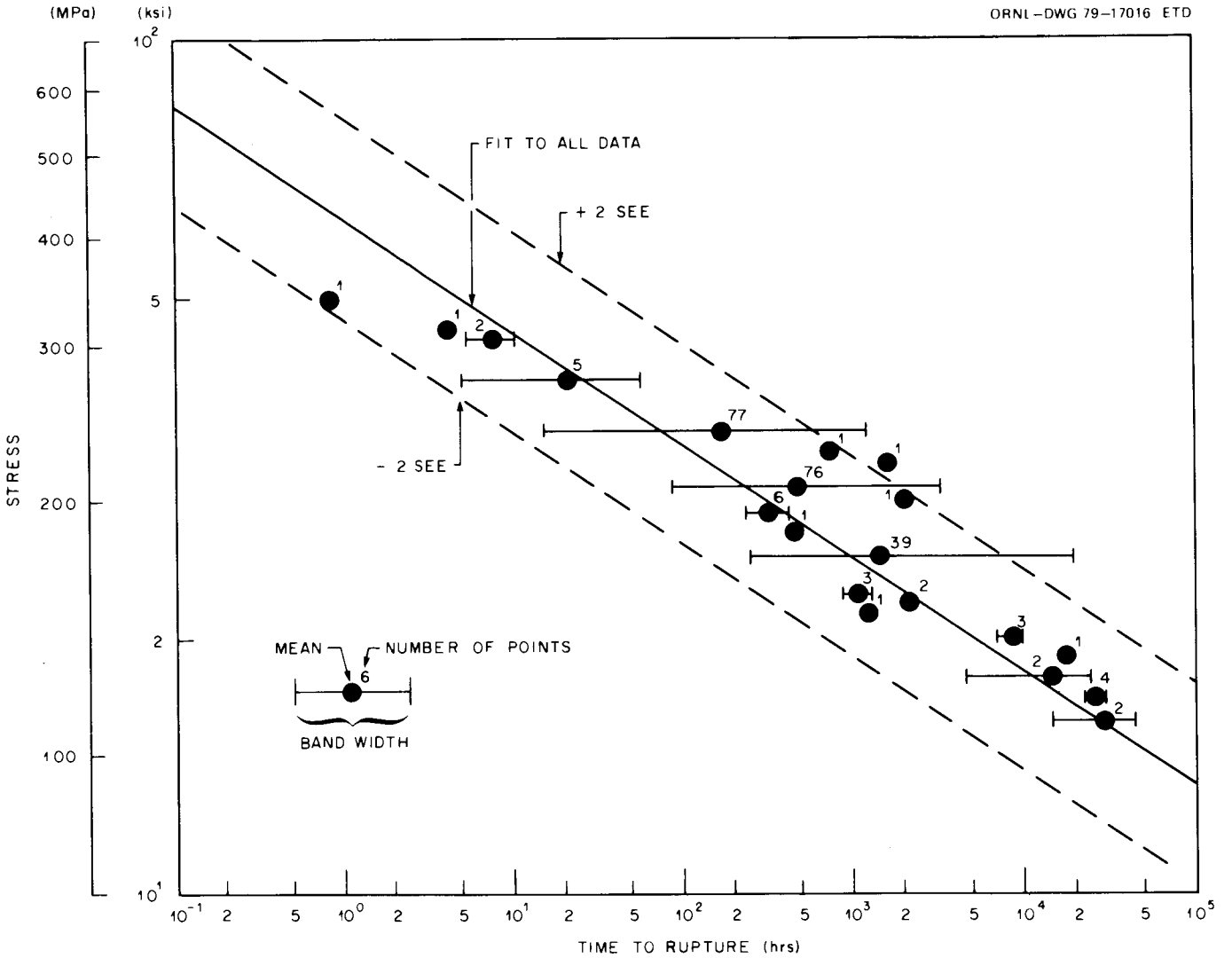

Fig. 14. Time-to-rupture vs stress at 593°C (1100°F) for 19 heats of type 304 stainless steel.

Table 8. Summary of results of least-squares fits[a] to time-to-rupture and minimum creep rate data

Property	Coefficients [MPa (ksi)]			
	$\bar{a}_1$	$\bar{a}_2$	R^2[b]	SEE
Time-to-rupture	7.24031×10^{19} (3.34556×10^{13})	−7.55519	0.96883	0.44118
Minimum creep rate	1.06345×10^{-24} (1.45649×10^{-16})	9.70335	0.90771	0.56634

[a]Fits were done to $\log_{10}$ form of power law.
[b]Correlation coefficient.

Table 9. Heat-to-heat variability of time-to-rupture function for type 304 stainless steel at 593°C (1100°F)

Heat identification No.	Time-to-rupture parameters		
	a_1 [MPa (ksi)]	B	SEE
1	8.6796×10^{19} (4.0107×10^{13})	1.19879	0.17706
3	3.8117×10^{19} (1.7613×10^{13})	0.52646	0.25924
4	7.9478×10^{19} (3.6725×10^{13})	1.09771	0.10852
5	7.9100×10^{19} (3.6550×10^{13})	1.09250	0.20015
6	1.9684×10^{20} (9.0954×10^{13})	2.71863	0.18858
7	2.8904×10^{20} (1.3356×10^{14})	3.99209	a
8	3.9873×10^{20} (1.8424×10^{14})	5.50711	0.25386
9	9.3064×10^{19} (4.3003×10^{13})	1.28536	0.15437
10	5.8601×10^{20} (2.7078×10^{14})	8.09370	0.29418
11	4.8939×10^{19} (2.2613×10^{13})	0.67592	0.23927
12	9.9983×10^{20} (4.6200×10^{14})	13.80919	0.09407
13	1.0206×10^{20} (4.7161×10^{13})	1.40964	0.17858
14	4.7172×10^{19} (2.1797×10^{13})	0.65152	0.25195
15	4.7969×10^{19} (2.2165×10^{13})	0.66253	0.25706
16	2.5284×10^{19} (1.1683×10^{13})	0.34921	0.20320
17	3.8644×10^{20} (1.7857×10^{14})	5.33740	0.39793
18	4.2627×10^{20} (1.9697×10^{14})	5.88743	0.25330
19	3.4534×10^{19} (1.5958×10^{13})	0.47697	0.11603
20	6.5076×10^{20} (3.0070×10^{14})	8.98796	0.15981

[a]Not enough data for statistical significance.

3.2.2 Creep deformation

The scope of this effort was not to develop new creep equations but to evaluate heat-to-heat variability using existing materials properties formulations wherever possible. A brief review of potential equations depicting creep behavior[1,24,25] indicated that the rational polynomial[25] was the most amenable for use in the heat-to-heat variability studies. The exponential formulation[1,24] has received wider exposure and verification, but the rational polynomial as used by Booker[25] offers a way of modeling material variability in creep without extensive fitting of creep curves. This, of course, assumes that the governing equations accurately capture the distribution, as well as the mean creep behavior.

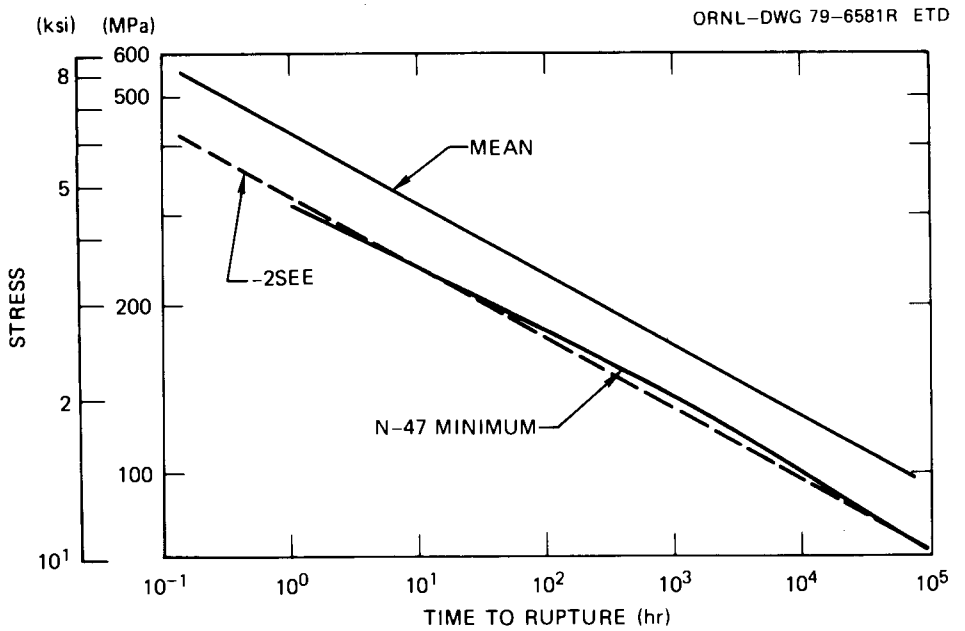

Fig. 15. Comparison of time-to-rupture correlation for 19 heats of type 304 stainless steel and ASME CCN47 design curve at 593°C (1100°F).

Following the development in Ref. 25, the rational polynomial equations for annealed type 304 stainless steel can be summarized as

$$\epsilon^c = \frac{Cpt}{1+pt} + \dot{\bar{\epsilon}}_m t \,, \tag{7}$$

$$C = 0.685\,(1.11\,\dot{\bar{\epsilon}}_m^{\,0.974} - \dot{\epsilon}_m)\bar{t}_r^{\,0.968} \,, \tag{8}$$

and

$$p = \frac{1}{C}\,(3.43\,\dot{\bar{\epsilon}}_m^{\,0.8} - \dot{\bar{\epsilon}}_m) \,, \tag{9}$$

where ϵ^c is total creep strain (%), $\dot{\bar{\epsilon}}_m$ is minimum creep rate (%/h), $\bar{t}_r$ is time-to-rupture (h), and t is time (h). The stress dependency of creep parameters C and p enters through the stress dependency of $\dot{\bar{\epsilon}}_m$ and $\bar{t}_r$.

In evaluating the limits on creep, at first all combinations of maxima and minima for $\dot{\bar{\epsilon}}_m$ and $\bar{t}_r$ seem to need consideration. However, there is a strong correlation between $\dot{\bar{\epsilon}}_m$ and $\bar{t}_r$ for the various heats, that is, heats that have lower minimum creep rates also have longer rupture lives (Fig. 13). Thus, realistic limits can be established for creep deformation of type 304 stainless steel from Eq. (7) by calculating C and p using only the combinations $[(\dot{\bar{\epsilon}}_m)_{max}, (\bar{t}_r)_{min}]$ and $[(\dot{\bar{\epsilon}}_m)_{min}, (\bar{t}_r)_{max}]$.

Minimum creep rate data, analogous to time-to-rupture data, were treated using a power law formulation

$$\dot{\bar{\epsilon}}_m = \bar{a}_1 \sigma^{\bar{a}_2} \,,$$

where $\dot{\bar{\epsilon}}_m$ is mean minimum creep rate for all heats (%/h) and $\bar{a}_1$, $\bar{a}_2$ are regression coefficients. At 593° C, 232 data points on 19 heats of material were analyzed, yielding the results shown in Table 8 and Fig. 16.

Heat-to-heat variability was treated like that for time-to-rupture. Thus,

$$\begin{aligned} \log (\dot{\epsilon}_m)_{\text{heat}} &= \log \dot{\bar{\epsilon}}_m + \log E_{\text{heat}} \\ &= \log (\bar{a}_1 E_{\text{heat}}) + \bar{a}_2 \log \sigma \\ &= \log a_1 + \bar{a}_2 \log \sigma \, . \end{aligned} \tag{10}$$

These results are summarized in Table 10.

Table 10. Heat-to-heat variability of minimum creep rate function for type 304 stainless steel at 593° C (1100° F)

Heat identification No.	Minimum creep rate parameters		
	a_1 [MPa (ksi)]	E	SEE
1	8.8441×10^{-25} (1.2113×10^{-16})	0.83164	0.21290
3	1.9532×10^{-24} (2.6751×10^{-16})	1.83666	0.23888
4	1.4585×10^{-24} (1.9975×10^{-16})	1.37144	0.08776
5	8.3737×10^{-25} (1.1469×10^{-16})	0.78742	0.20161
6	1.4743×10^{-25} (2.0191×10^{-17})	0.13863	0.24565
7	1.0009×10^{-25} (1.3708×10^{-17})	0.09412	[a]
8	8.6578×10^{-26} (1.1858×10^{-17})	0.08141	0.17640
9	7.8253×10^{-25} (1.0717×10^{-16})	0.73585	0.24299
10	1.3349×10^{-25} (1.8283×10^{-17})	0.12553	0.39129
11	1.7138×10^{-24} (2.3471×10^{-16})	1.61151	0.16488
12	4.2556×10^{-26} (5.8284×10^{-18})	0.04002	0.09957
13	6.0676×10^{-25} (8.3101×10^{-17})	0.57056	0.17112
14	1.6944×10^{-24} (2.3206×10^{-16})	1.59323	0.30595
15	1.2386×10^{-24} (1.6964×10^{-16})	1.16470	0.23212
16	6.4415×10^{-24} (2.7898×10^{-15})	19.15453	0.95311
17	1.7827×10^{-25} (2.4415×10^{-17})	0.16763	0.50301
18	1.0869×10^{-25} (1.4886×10^{-17})	0.10221	0.46285
19	5.4042×10^{-24} (7.4015×10^{-16})	5.08178	0.05322
20	1.0634×10^{-25} (1.4565×10^{-17})	0.10000	0.23285

[a]Not enough data for statistical significance.

Using the materials deformation equations summarized above and PLACRE,[26] a number of preliminary one-dimensional inelastic pipe ratchetting analyses were performed. The selected structure geometry and load conditions were based on test TTT-1 (Ref. 27). Results from these preliminary analyses underpredicted the measured ratchetting strains by large margins. Thus, before performing the full set of analyses, the decision was made to give additional attention to the recommended materials correlations to determine if characteristics of the individual equations (i.e., form chosen, extrapolation properties) could be causing the difficulty.

As observed from the preliminary analyses, creep strain prediction seemed to have a dominate role in predicting ratchetting strain. Because TTT-1 was being used as the benchmark for these calculations, a comparison was made with the recommended rational polynomial equation [adjusted to heat 14

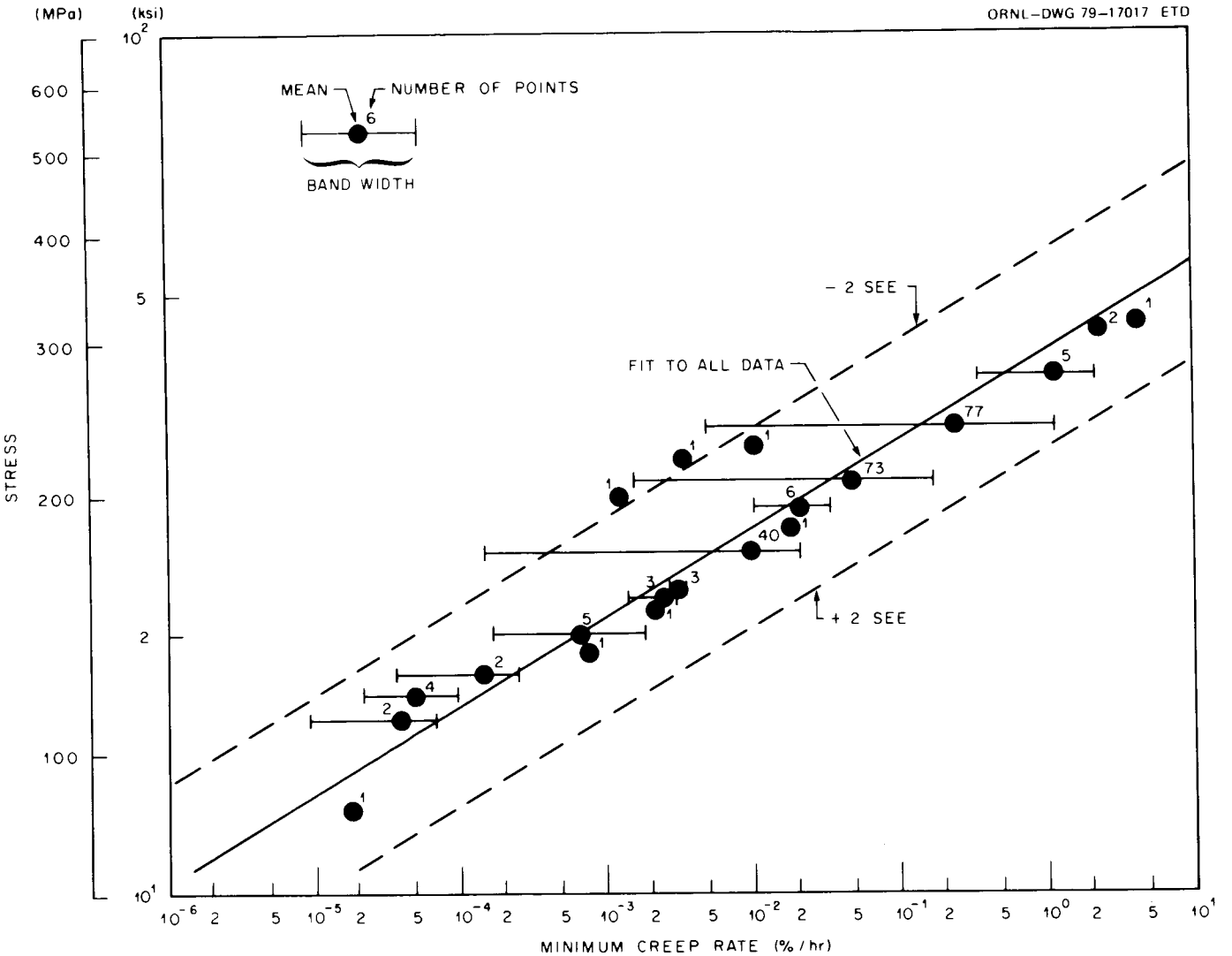

Fig. 16. Minimum creep rate vs stress at 593°C (1100°F) for 19 heats of type 304 stainless steel.

(ORNL ref. HT 9T2796)] and the creep data matrix developed explicitly for this heat (Table 11). This data matrix was developed from data on ~30 creep tests and validated through inelastic analyses of a number of structures. The conclusion was reached that this matrix would be used as a standard of comparison for evaluating the final rational polynomial equation to be used.

Compared on a percentage basis, the rational polynomial equation differed significantly from the matrix at stresses less than 103 MPa (15 ksi) and times less than about 1000 h (Fig. 17), although at higher stresses and longer times excellent agreement was obtained. The preliminary structural analyses indicated that the stress in the model was in the range 55 to 83 MPa (8 to 12 ksi). Thus, the structural stresses were in a range of poorest agreement between experimental data and the creep equation.

When the input parameters to the rational polynomial creep equation were considered, minimum creep rate had the most significant effect on calculated creep. Also, higher creep strains would be predicted at low stresses if minimum creep rates were used that were larger than those calculated by the power law fit to the high stress data. This led to consideration of the hyperbolic sine form of equation for extrapolating minimum creep rate to low stresses.

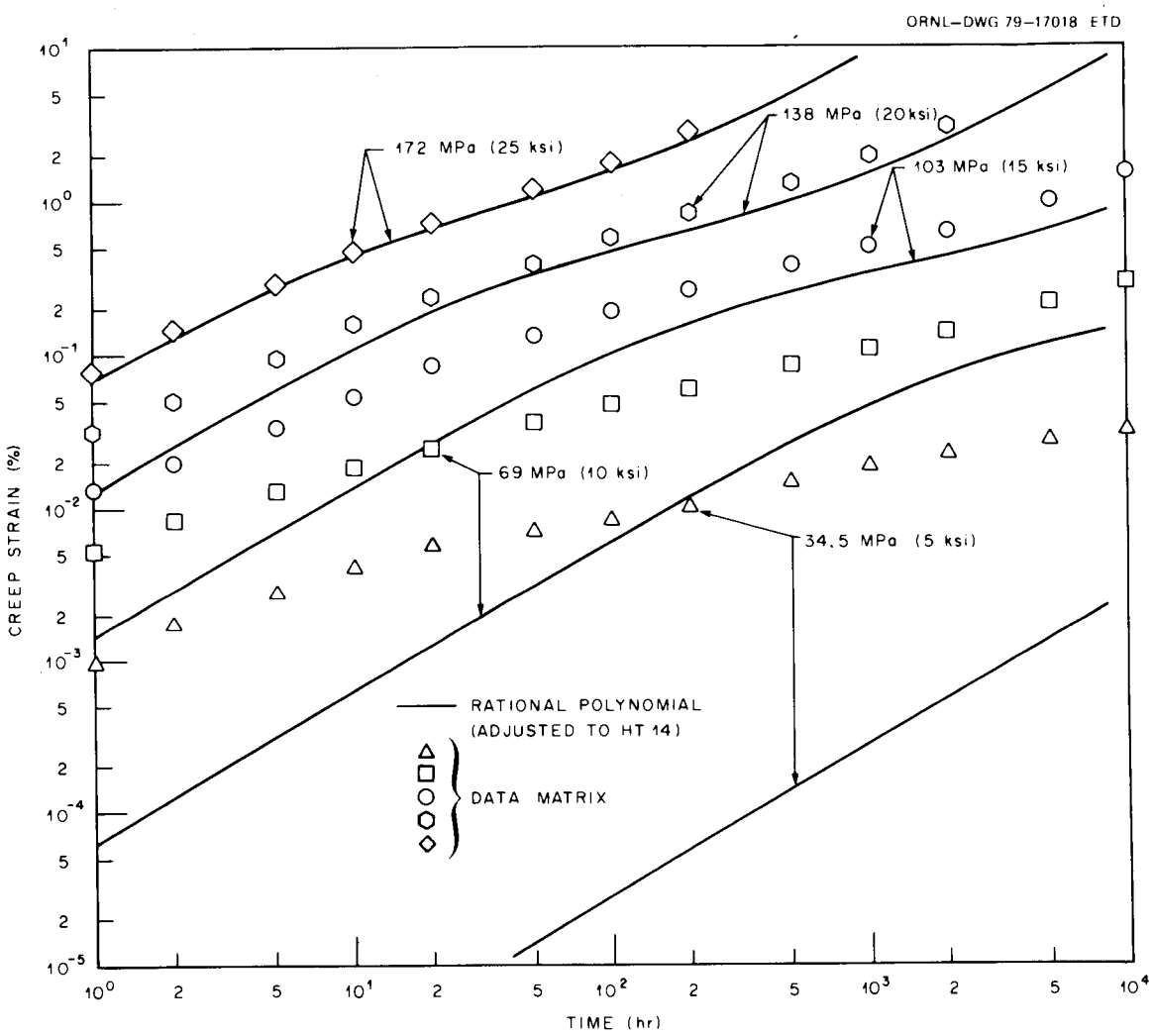

Fig. 17. Comparison of creep data matrix with predicted creep strain for heat 14 using the rational polynomial equation with power law representations of ϵ_m and t_r.

Table 11. Uniaxial creep strain (%) matrix for type 304 stainless steel (heat 9T2796) at 593° C (1100° F)

Stress (ksi)	Time (h)												
	1	2	5	10	20	50	100	200	500	1000	2000	5000	10,000
1	0.00006	0.00010	0.00022	0.00040	0.00060	0.00067	0.00078	0.00098	0.00150	0.00200	0.00250	0.00320	0.00370
2	0.00018	0.00032	0.00065	0.00100	0.00140	0.00170	0.00210	0.00270	0.00400	0.00470	0.00550	0.00700	0.00800
3	0.00036	0.00070	0.00120	0.00182	0.00250	0.00300	0.00355	0.00450	0.00700	0.00830	0.01000	0.01200	0.01400
4	0.00060	0.00115	0.00187	0.00280	0.00400	0.00475	0.00575	0.00750	0.01000	0.01250	0.01500	0.01900	0.02150
5	0.00095	0.00173	0.00275	0.00410	0.00570	0.00700	0.00830	0.01010	0.01500	0.01870	0.02250	0.02750	0.03150
6	0.00140	0.00250	0.00400	0.00575	0.00775	0.00980	0.01200	0.01600	0.02220	0.02750	0.03200	0.03950	0.04500
7	0.00210	0.00355	0.00550	0.00800	0.01070	0.01375	0.01700	0.02250	0.03100	0.03800	0.04700	0.05800	0.06700
8	0.00290	0.00485	0.00765	0.01070	0.01450	0.01950	0.02400	0.03100	0.04300	0.05300	0.06800	0.08900	0.10500
9	0.00400	0.00650	0.01000	0.01400	0.01900	0.02650	0.03300	0.04350	0.06000	0.07500	0.10100	0.14000	0.16500
10	0.00515	0.00830	0.01300	0.01815	0.02400	0.03600	0.04700	0.06000	0.08300	0.10700	0.14000	0.21500	0.29000
11	0.00650	0.01035	0.01650	0.02300	0.03150	0.04900	0.06500	0.08500	0.12000	0.15300	0.19500	0.31250	0.50000
12	0.00750	0.01240	0.02000	0.02900	0.04200	0.06500	0.08900	0.11500	0.16500	0.21000	0.27000	0.43750	0.68000
13	0.00910	0.01475	0.02450	0.03600	0.05400	0.08500	0.11700	0.15500	0.22000	0.28500	0.37200	0.57500	0.90000
14	0.01150	0.01720	0.02800	0.04200	0.06750	0.10750	0.15200	0.20250	0.29500	0.38000	0.49400	0.75500	1.16500
15	0.01355	0.01965	0.03350	0.05300	0.08500	0.13350	0.19100	0.25950	0.38000	0.49300	0.62500	0.98500	1.48000
16	0.01515	0.02220	0.03800	0.06100	0.10300	0.16500	0.24200	0.32250	0.48000	0.62500	0.80000	1.25000	1.90000
17	0.01700	0.02450	0.04500	0.07200	0.11600	0.20250	0.29800	0.39400	0.60000	0.80000	1.04500	1.60000	2.50000
18	0.02500	0.03500	0.05600	0.08600	0.14000	0.24000	0.35500	0.51000	0.77500	1.05000	1.40000	2.20000	3.50000
19	0.02800	0.04200	0.08000	0.12500	0.19000	0.30000	0.45000	0.65000	0.99000	1.40000	2.00000	2.97500	
20	0.03200	0.05000	0.09500	0.16000	0.24000	0.38500	0.57500	0.82000	1.27500	1.95000	3.00000		
21	0.03600	0.06000	0.12200	0.20000	0.31000	0.49000	0.71000	1.02500	1.67500	2.70000			
22	0.04000	0.07700	0.15500	0.25000	0.39000	0.62000	0.88500	1.31000	2.25000				
23	0.05000	0.09500	0.19500	0.31000	0.48000	0.77500	1.11100	1.68500	3.00000				
24	0.06500	0.12000	0.23500	0.38000	0.60000	0.95500	1.40000	2.17500					
25	0.08000	0.15000	0.29000	0.47000	0.72500	1.20000	1.77500	2.80000					
26	0.09000	0.17700	0.35000	0.57500	0.90000	1.51000	2.25000	3.50000					
27	0.11500	0.22000	0.42300	0.70000	1.10000	1.90000	2.80000						
28	0.14500	0.26000	0.50000	0.85000	1.35500	2.34000	3.42000						
29	0.18000	0.32500	0.61500	1.03500	1.68000	2.87500							
30	0.22500	0.40000	0.77000	1.25500	2.07500	3.42500							
31	0.28000	0.50500	0.98000	1.54500	2.55000								
32	0.35000	0.63200	1.25000	1.90000	3.06500								
33	0.43500	0.80000	1.57500	2.31000									
34	0.53500	0.98000	1.92500	2.80000									
35	0.65500	1.21500	2.31000	3.32500									

A procedure following that of Blackburn[24] was used to develop the required equation. The final recommended form was

$$\dot{\bar{\epsilon}}_m = \bar{a}_1 \sin\left(\frac{\bar{a}_2\sigma}{\bar{a}_3}\right)^{a_3}, \tag{11}$$

where

$\dot{\bar{\epsilon}}_m$ = minimum creep rate (%/h),

σ = stress (MPa),

$\bar{a}_1 = 2.7566 \times 10^{-5}$,

$\bar{a}_2 = 0.05416$,

$\bar{a}_3 = 5.32$,

with a standard error of 0.5584. This correlation, based on all data, is shown in Fig. 18. The hyperbolic sine was used as exemplifying one method of extrapolation that has previously been used with success. Using the hyperbolic sine form for $\dot{\bar{\epsilon}}_m$, the greatest change in the shape of the function is in the low-to-medium stress region (<150 MPa) where data become scarce (Fig. 18). Some degree of uncertainty is thus introduced in both representing the low and medium stress data and, particularly, in extrapolation to the lower stress levels calculated in the preliminary structural analyses. Noting also the strong correlation between minimum creep rate and time-to-rupture (Fig. 13), the equation

$$\bar{t}_r = \bar{b}_1(\dot{\bar{\epsilon}}_m)^{b_2}, \tag{12}$$

where

$\bar{t}_r$ = time-to-rupture (h),

$\bar{b}_1 = 16.9256$,

$\bar{b}_2 = -0.7639$,

with a standard error of 0.17155 was also recommended.

Using Eqs. (11) and (12), a comparison of predicted creep strain for heat 14 using the rational polynomial and the data matrix is shown in Fig. 19. An improvement in agreement has been achieved in the low stress–short time regions noted above. Further improvement seemed to be beyond the capability of the rational polynomial using an equation of only one term (or any other of the candidate creep equation forms using only one term).

Comparing the predicted minimum time-to-rupture using Eqs. (11) and (12) with the ASME CCN47 minimum curve (Fig. 20), agreement is not as good as for the power law representation. At the stress and time levels of interest for this study, the difference could be as much as a factor of 4.

Using these recommended materials properties, a series of 18 one-dimensional inelastic pipe ratchetting analyses were carried out with the finite-element program PLACRE. A reference analysis was also performed using material properties in Refs. 1 and 2. The same structure geometry and load conditions were used as in the preliminary analyses (i.e., based on TTT-1) (Fig. 1).

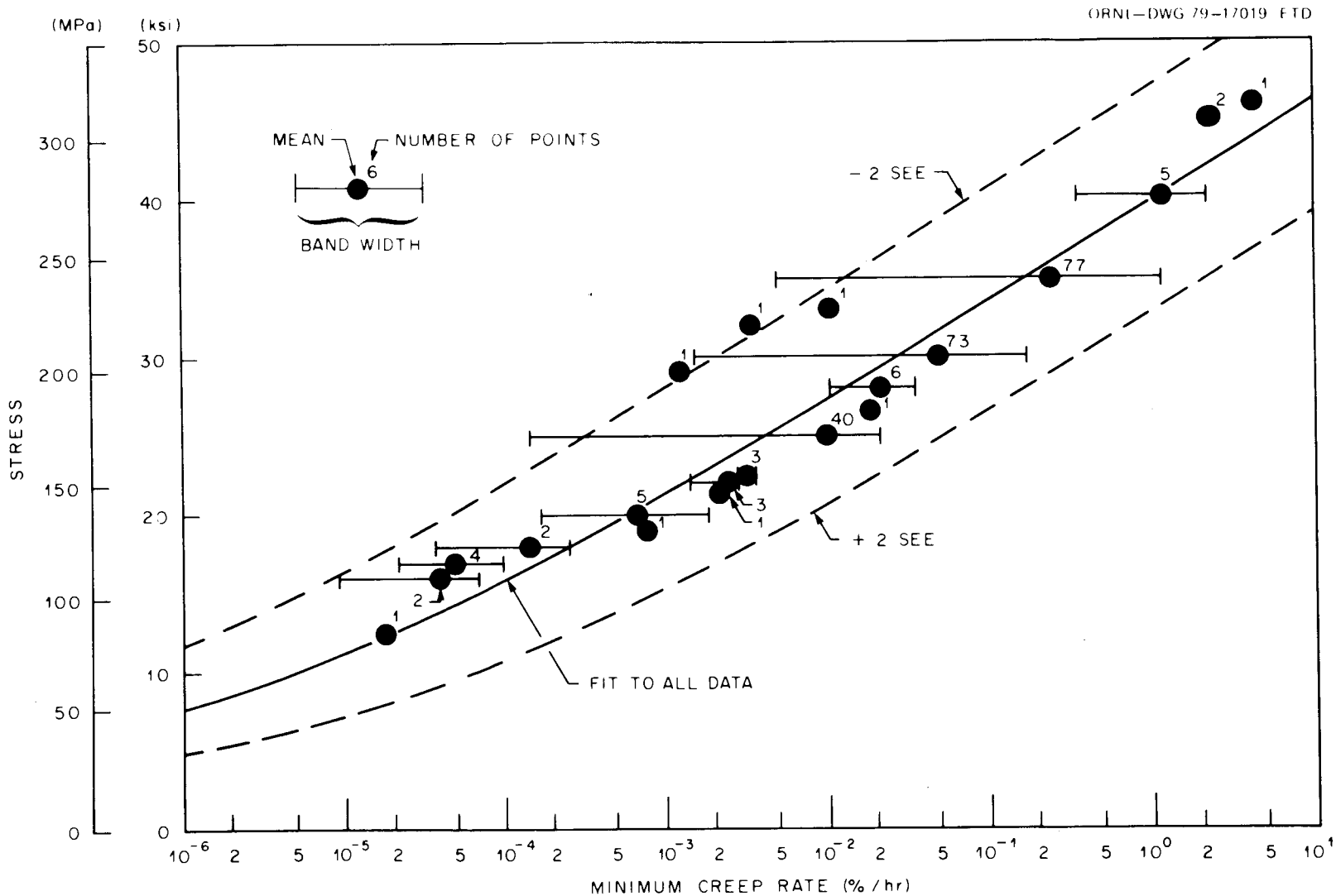

Fig. 18. Hyperbolic sine correlation of minimum creep rate data vs stress at 593° C (1100° F) for 19 heats of type 304 stainless steel.

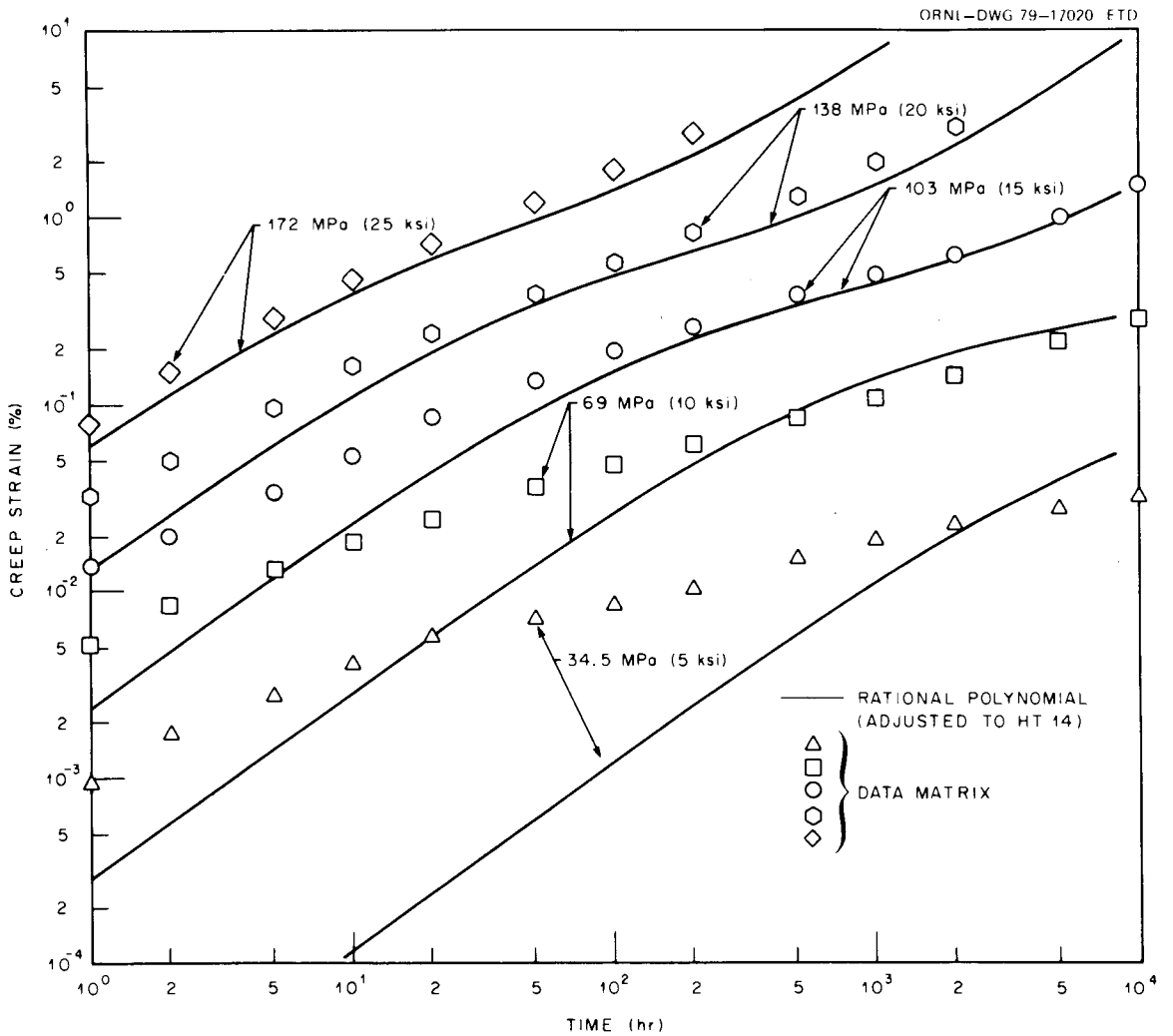

Fig. 19. Comparison of creep data matrix with predicted creep strain for heat 14 using the rational polynomial equation with hyperbolic sine represen tation of ϵ_m and t_r.

Results of these analyses indicated that the reference analysis would be nonconservative in both predicted ratchetting strain and creep damage when compared with the heat variability analyses. For ratchetting strain, nonconservatism was not considered surprising because (1) no safety factors were incorporated into the reference analysis procedures that were followed and (2) overrunning of the strain limits does not necessarily indicate structural failure.

Nonconservatism for creep damage was considered more serious and was therefore investigated further. Most of the predicted creep damage nonconservatism could be attributed to a significantly lower time-to-rupture predicted by the hyperbolic sine form correlation of time-to-rupture compared to the design curve of CCN47 (Fig. 20). Further investigation revealed that the lower predicted time-to-rupture could not be satisfactorily justified by the data on which the present correlations were based but was more attributable to the form adopted for the equations. Obviously, the initial power law formulation for time-to-rupture would give more consistent results with respect to evaluating creep damage.

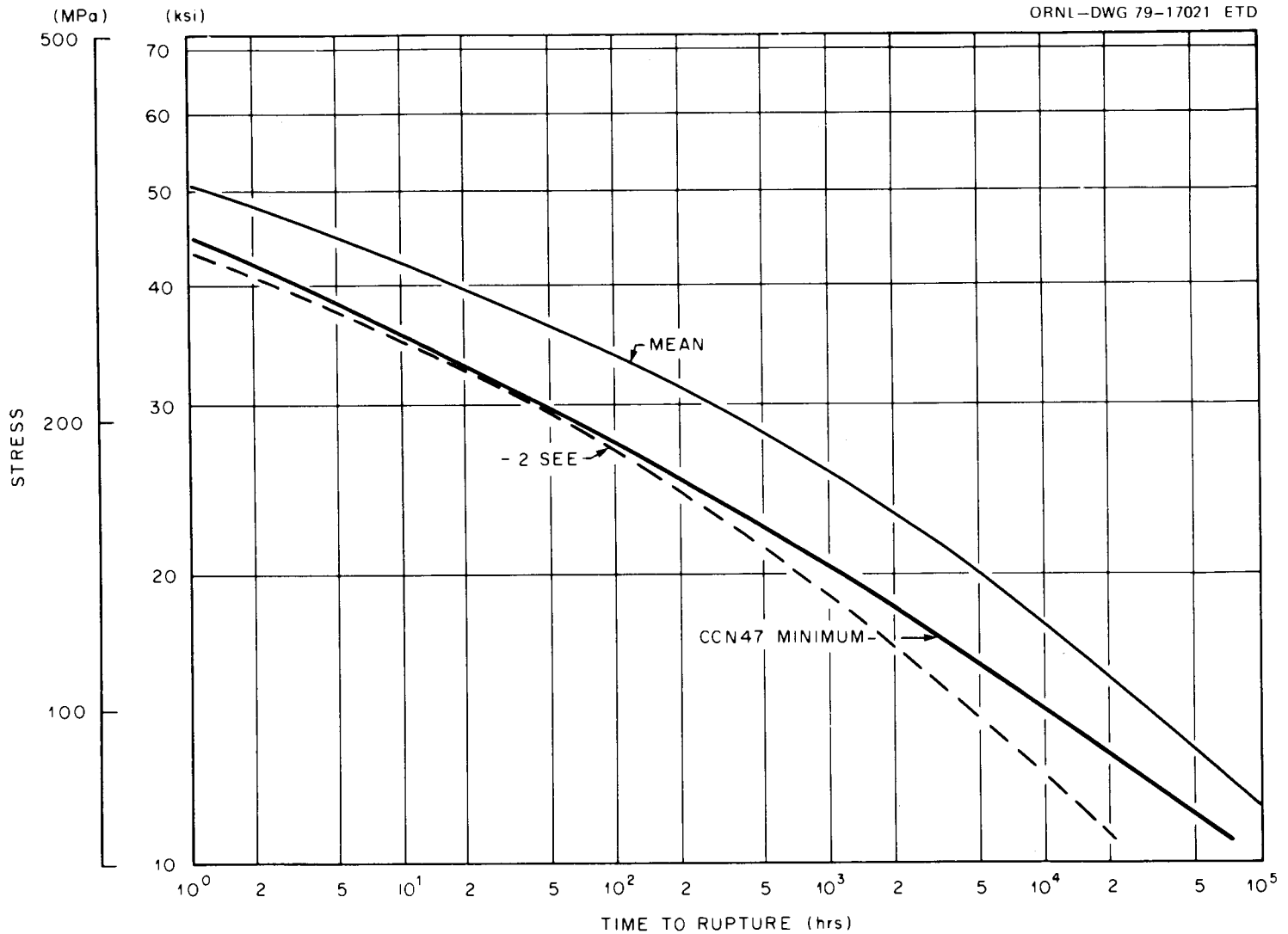

Fig. 20. Comparison of time-to-rupture correlation for 19 heats of type 304 stainless steel using the hyperbolic sine representation with ASME CCN47 design curve at 593°C (1100°F).

Utilization of the power law form for time-to-rupture in conjunction with the hyperbolic sine form for minimum creep rate would introduce inconsistencies in the data representations. An alternate approach would be to use the power law correlations for $\dot{\bar{\epsilon}}_m$ and $\bar{t}_r$ and modify the creep equation. This approach was adopted.

In keeping with the criterion that the data matrix (Table 10) would be used as a standard for creep deformation, the rational polynomial equation was disregarded and a three-exponential creep equation[28] was used instead. Material (heat) dependency could be incorporated in this equation by modifying it to reflect the rational polynomial development. Specifically, constants in the three-exponential equation could be formulated in terms of the calculated parameters C and p, which were heat dependent.

The three-exponential equation developed in standard English units for ORNL reference heat 14 is

$$\epsilon^c = A_1 \times [1 - \exp(-R_1 \times t)] + A_2 \times [1 - \exp(-R_2 \times t)] + A_3 \times [1 - \exp(-R_3 \times t)] + \dot{\bar{\epsilon}}_m \times t \,, \qquad (13)$$

where

$$A_1 = (5.933 \times 10^{-4}) \times \sigma,$$

$$A_2 = (8.3524 \times 10^{-4}) \times \sigma^{1.8766},$$

$$A_3 = (2.849 \times 10^{-5}) \times \sigma^{3.6966},$$

$$R_1 = 9.4045 \times 10^{-2} \times \exp(0.214454 \times \sigma),$$

$$R_2 = 2.7495 \times 10^{-3} \times \exp(0.17537 \times \sigma),$$

$$R_3 = 1.0928 \times 10^{-4} \times \exp(0.11757 \times \sigma),$$

$$\dot{\epsilon}_m = \begin{cases} 6.49 \times 10^{-7} \times [\sinh(0.1491 \times \sigma)]^3 \text{ for } \sigma \leqslant 25.932 \text{ ksi} \\ 2.968 \times 10^{-6} \times [\sinh(0.17116 \times \sigma)]^{2.13562} \text{ for } \sigma > 25.932 \text{ ksi.} \end{cases}$$

In this equation, σ is in thousands of pounds per square inch (ksi), ϵ is in percent, t is in hours, and $\dot{\epsilon}_m$ is in percent per hour. A comparison of this equation with the data in Table 10 is shown in Fig. 21. As can be seen, the fit is acceptable over a wide range of stresses, times, and creep strains.

The method of modifying Eq. (13) to reflect heat dependency follows. By establishing equivalency of initial creep rate and magnitude of primary creep strain between Eq. (7) and Eq. (13), the constants in Eq. (13) could be implicitly expressed in terms of C and p. Thus, the magnitude of primary creep strain should be the same in each equation. Then

$$\sum_{i=1}^{3} A_i = C \,. \qquad (14)$$

Let (*) denote a reference state, in this case the ORNL reference heat. With minor rearranging

$$\sum_{i=1}^{3} \frac{A_i^*}{C^*} = 1 \,.$$

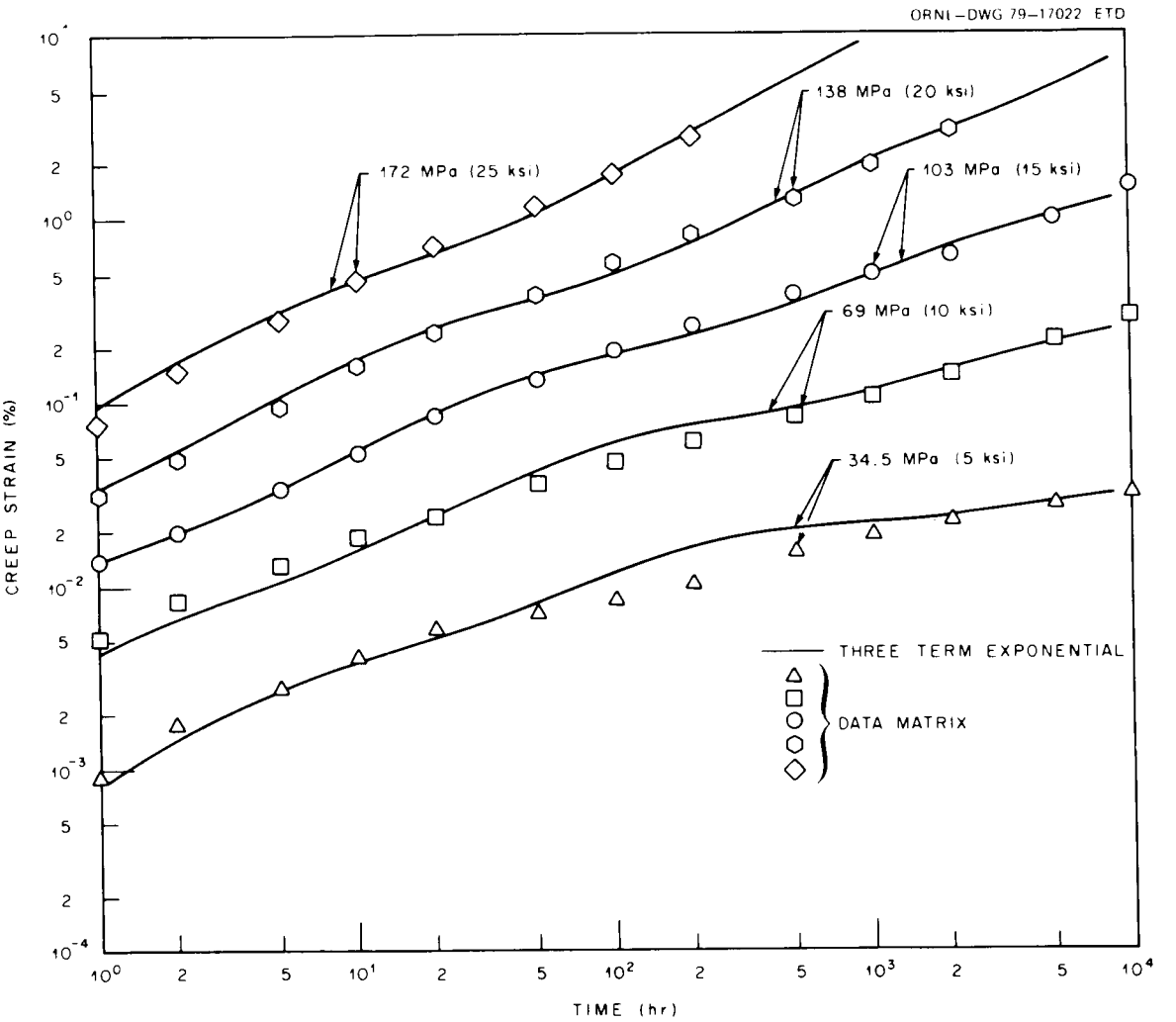

Fig. 21. Comparison of a three-exponential equation for uniaxial creep with creep data over a stress range of 34.5 to 241 MPa (5 to 35 ksi) (1 ksi = 6.895 MPa) for type 304 stainless steel (ORNL reference heat) at 593°C (1100°F).

For any other state (or heat), Eq. (14) also applies, and

$$C \sum_{i=1}^{3} \frac{A_i^*}{C^*} = C ,$$

or

$$\sum A_i^* \frac{C}{C^*} = C . \tag{15}$$

One state of equivalency between Eqs. (14) and (15) is when

$$A_i = A_i^* \frac{C}{C^*} . \tag{16}$$

A comparable development using initial creep rate will lead to

$$R_i = R_i^* \frac{p}{p^*} \ . \tag{17}$$

These results are applied as follows. The A_i^* and R_i^* are reference values in Eq. (18). The C^* and p^* are reference parameters calculated for the reference heat using Eqs. (8) and (9). Equations (12) and (10) are used to calculate t_r and $\dot{\epsilon}_m$ respectively. For any other heat (or mean value), the applicable C and p values are calculated, A_i and R_i are formulated, and the creep behavior is predicted through Eq. (13). Limits on creep deformation (i.e., maximum and minimum) are incorporated through the limits on t_r and $\dot{\epsilon}_m$. As discussed previously, ϵ^c_{max} corresponds to $[(\dot{\epsilon}_m)_{max}, (t_r)_{min}]$ and ϵ^c_{min} corresponds to $[(\dot{\epsilon}_m)_{min}, (t_r)_{max}]$.

As a check, Eqs. (13), (16), and (17) were applied to heat 14. Figure 22 shows a comparison between the data matrix and the calculated creep strain; the comparison is very credible.

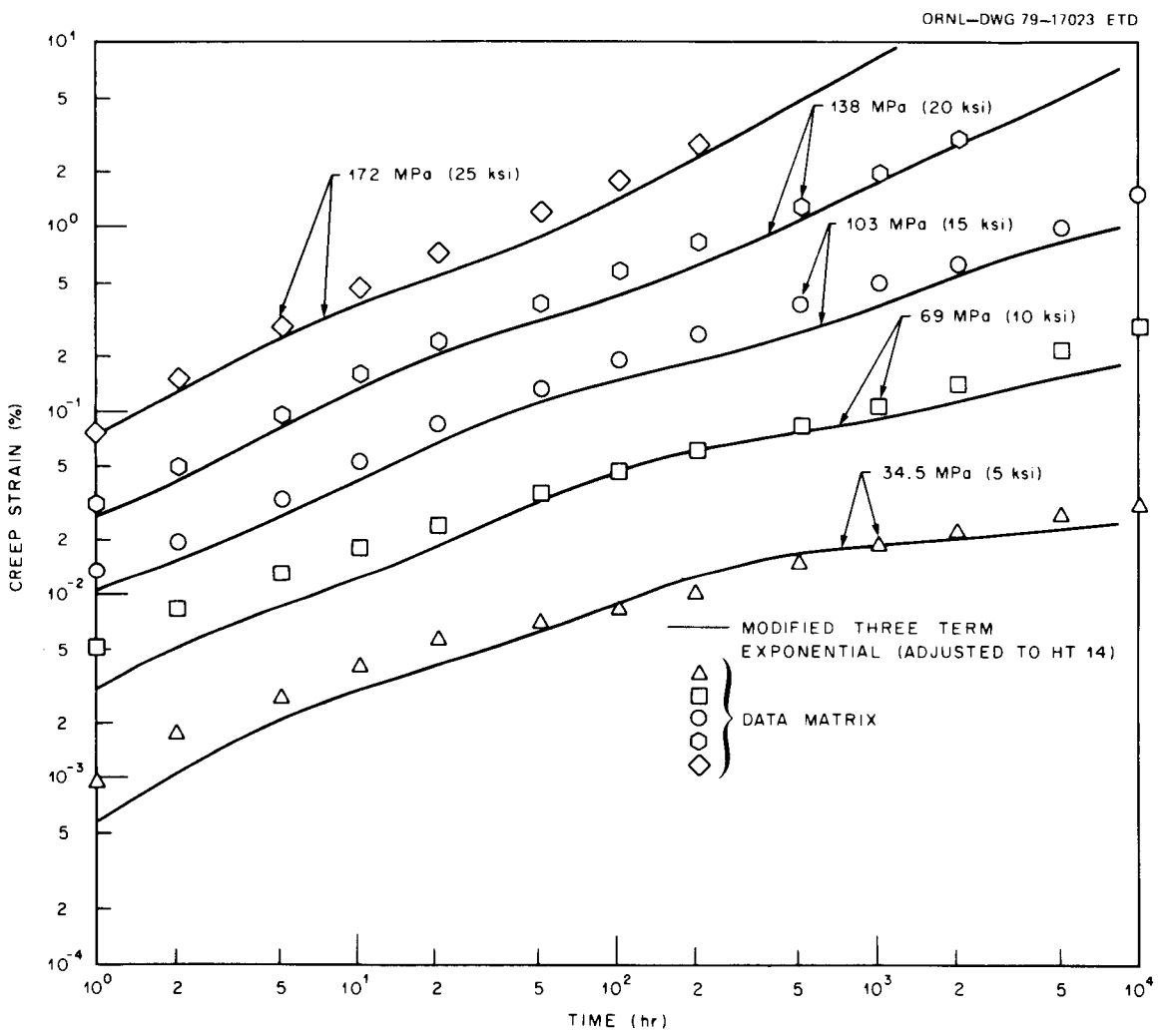

Fig. 22. Comparison of creep data matrix with predicted creep strain for heat 14 using the modified three-exponential equation with power law representation of ϵ_m and t_r.

3.3 Fatigue Properties

In considering fatigue properties, reliance on previous work was essential because of complexity of fatigue behavior description. Diercks and Raske[29] performed a thorough statistical analysis of the then-available data on type 304 stainless steel. With respect to heat-to-heat variability, for continuous cycling, they concluded that there were no statistically significant differences in the data from the different heats.

For zero hold-time conditions to be used in the structural analyses, the formulation proposed in Ref. 29 reduces to

$$(\log_{10} N_f)^{-1/2} = 1.2055 + 0.6600S + 0.1804S^2 - 0.008143S^4 + (2.53 \times 10^{-4})RS^4 + (2.18 \times 10^{-4})TS^4 - (5.466 \times 10^{-4})RT^2 .$$

Here

$$S = \log_{10} (\Delta\epsilon_t / 100),$$

$$R = \log_{10} (\dot{\epsilon}),$$

$$T = T_c / 100,$$

where

N_f = cycles to failure,

$\Delta\epsilon_t$ = total strain range (%),

$\dot{\epsilon}$ = strain rate (s^{-1}),

T_c = temperature (° C).

Using the approach adopted for the variability study along with this equation, analyses were performed using the available data and

$$(\log N_f)_{heat}^{-1/2} = (\log \overline{N_f})^{-1/2} + N_{heat} ;$$

little discernable difference between heats could be detected. Thus, no fatigue heat-to-heat variability was recommended for consideration in the structural analyses.

3.4 Discussion of Cross Correlations

As discussed previously, cross correlations between properties were of interest both as a means of "constructing" data sets where limited data were available for a given property and as a means of reducing the total number of random variables to be considered in the inelastic analyses. The most convenient way of studying potential cross correlations was to compare the heat variability factors for different properties after fits for these properties were developed. If a correlation was apparent, then a more detailed investigation of the data would be pursued. This technique was employed in developing the heat-dependent creep equation discussed in Sect. 3.2 where minimum creep rate was correlated with time-to-rupture.

The properties that were of most interest were yield stress, ultimate stress, minimum creep rate, and time-to-rupture. Cross correlations of these properties had the greatest potential for reducing the number of random variables for the analyses (i.e., for reducing the total number of inelastic analyses required). Figures 23 and 24 show a comparison of the yield stress heat adjustment coefficient H with the minimum creep rate and time-to-rupture heat adjustment coefficients, E and B respectively. As can be seen, there are no clearly definable correlations with yield stress.

Figures 25 and 26 show a comparison of the ultimate strength heat adjustment coefficient F and the minimum creep rate and time-to-rupture heat adjustment coefficients, E and B respectively. Although

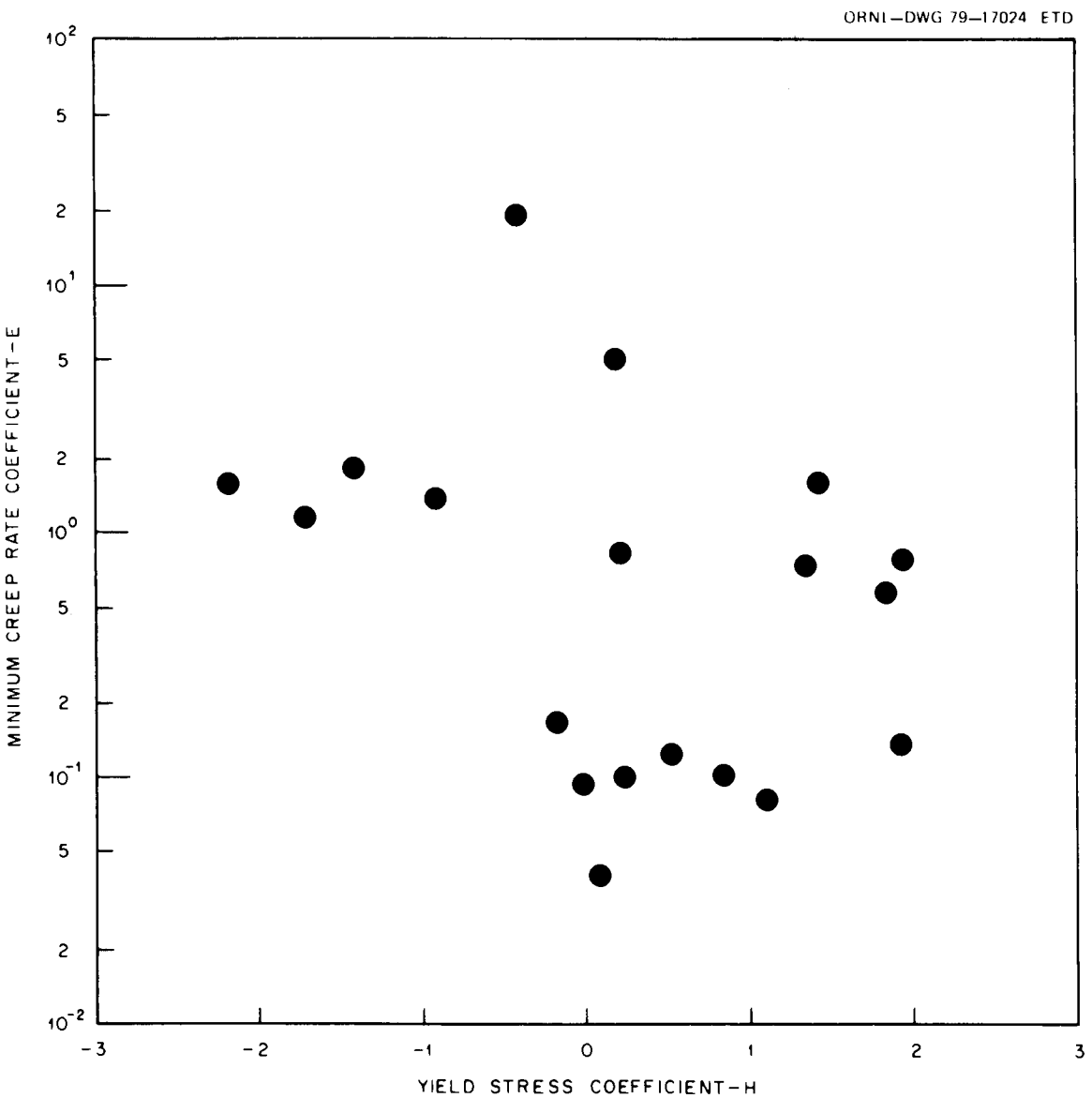

Fig. 23. Comparison of yield stress (0.2%) with minimum creep rate heat adjustment factors, H and E, for 19 heats of type 304 stainless steel.

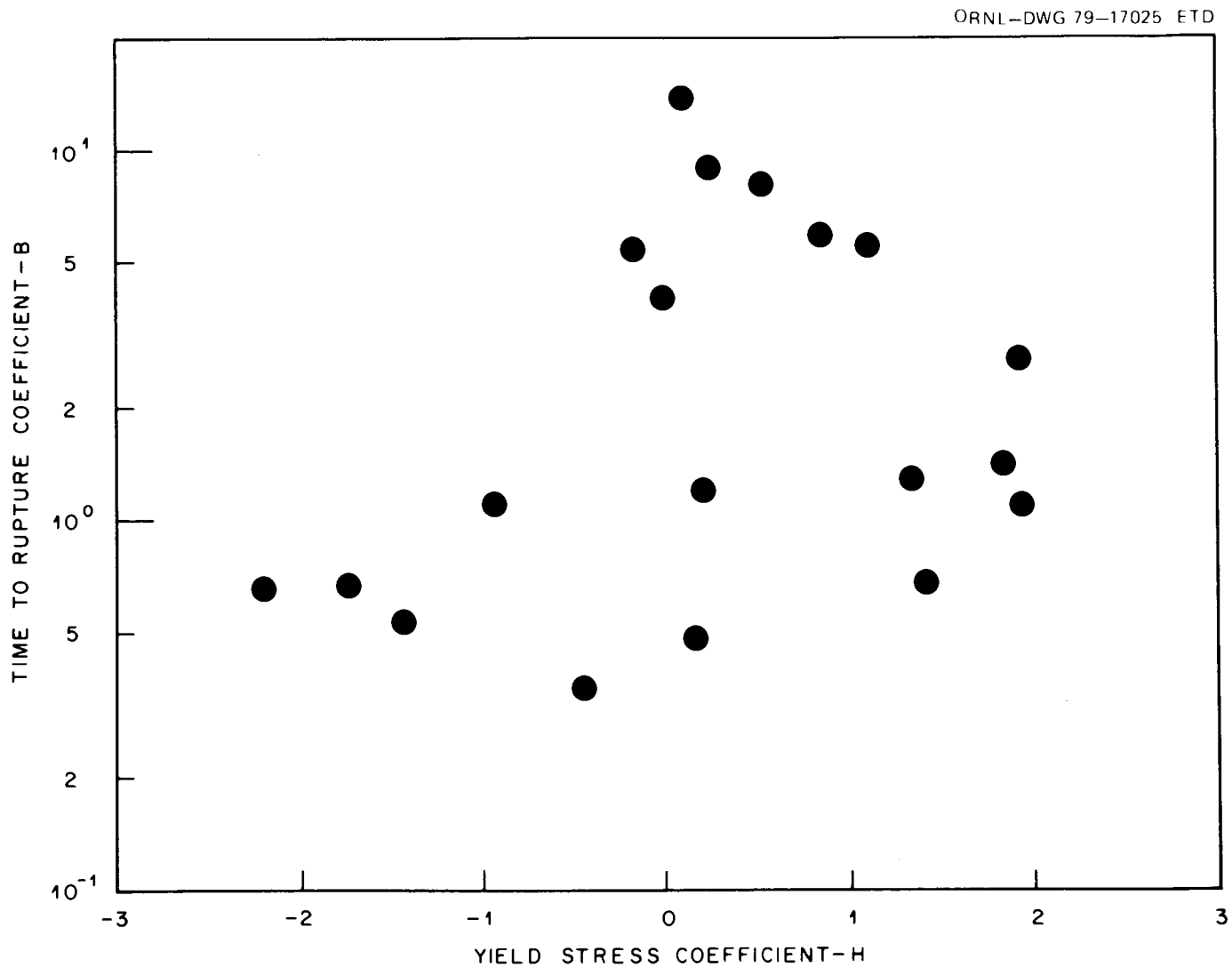

Fig. 24. Comparison of yield stress (0.2%) with time-to-rupture heat adjustment factors, H and B, for 19 heats of type 304 stainless steel.

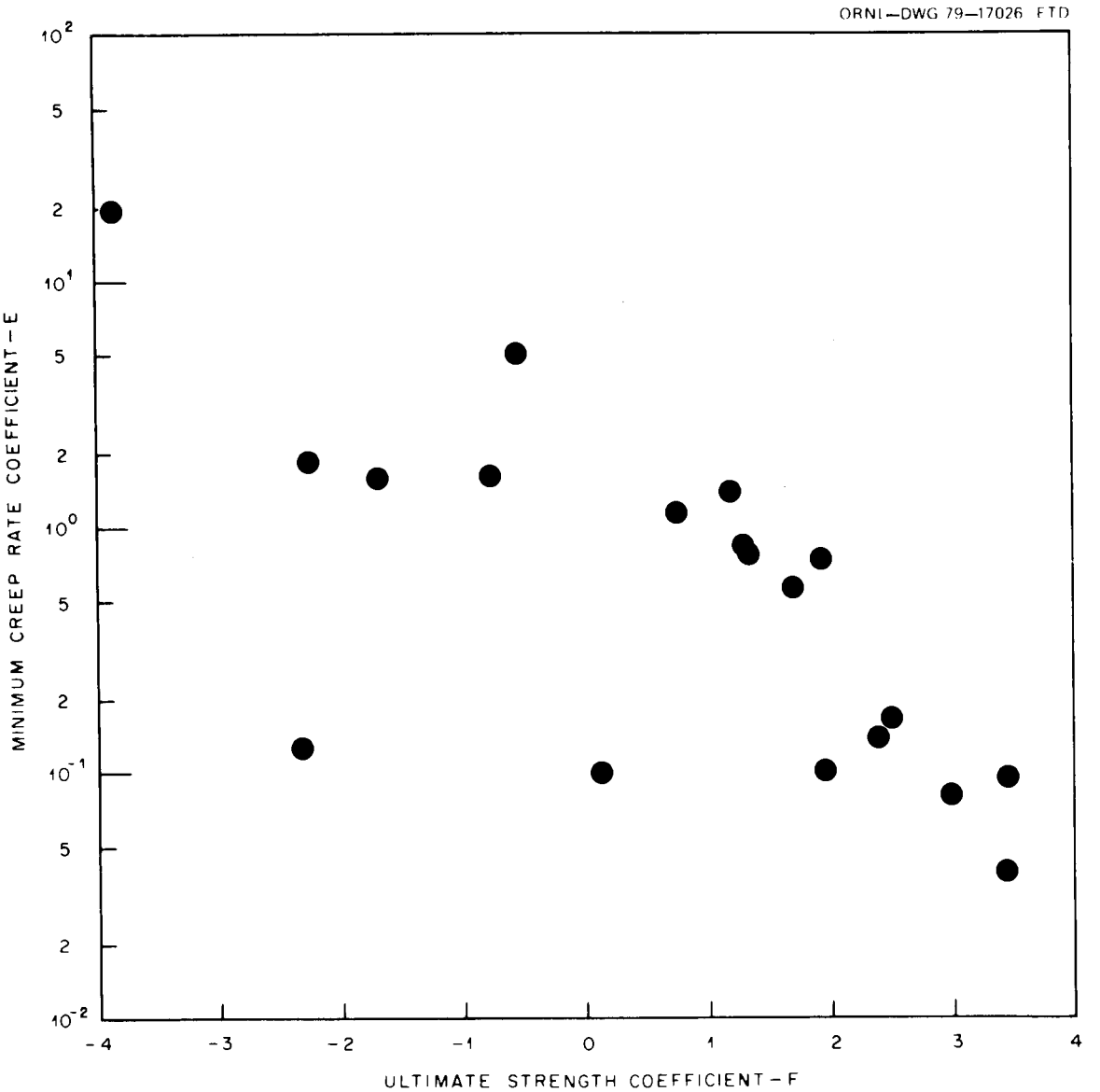

Fig. 25. Comparison of ultimate strength with minimum creep rate heat adjustment factors, F and E, for 19 heats of type 304 stainless steel.

there is a fair amount of scatter in these comparisons, a visual inspection would indicate some trend between F and E and F and B. This observation is in agreement with the work of Sikka et al.,[19] who were able to correlate creep properties with ultimate strength. For this work, however, the complexities involved in trying to correlate ultimate strength with minimum creep rate and time-to-rupture were not felt to be warranted by any simplifications to be gained. Thus, these properties were considered independent of one another.

Figure 27 shows a comparison of minimum creep rate and time-to-rupture heat adjustment coefficients, E and B; a strong relationship between these two properties is evident. The resulting correlation is shown in Fig. 13, Sect. 3.2.

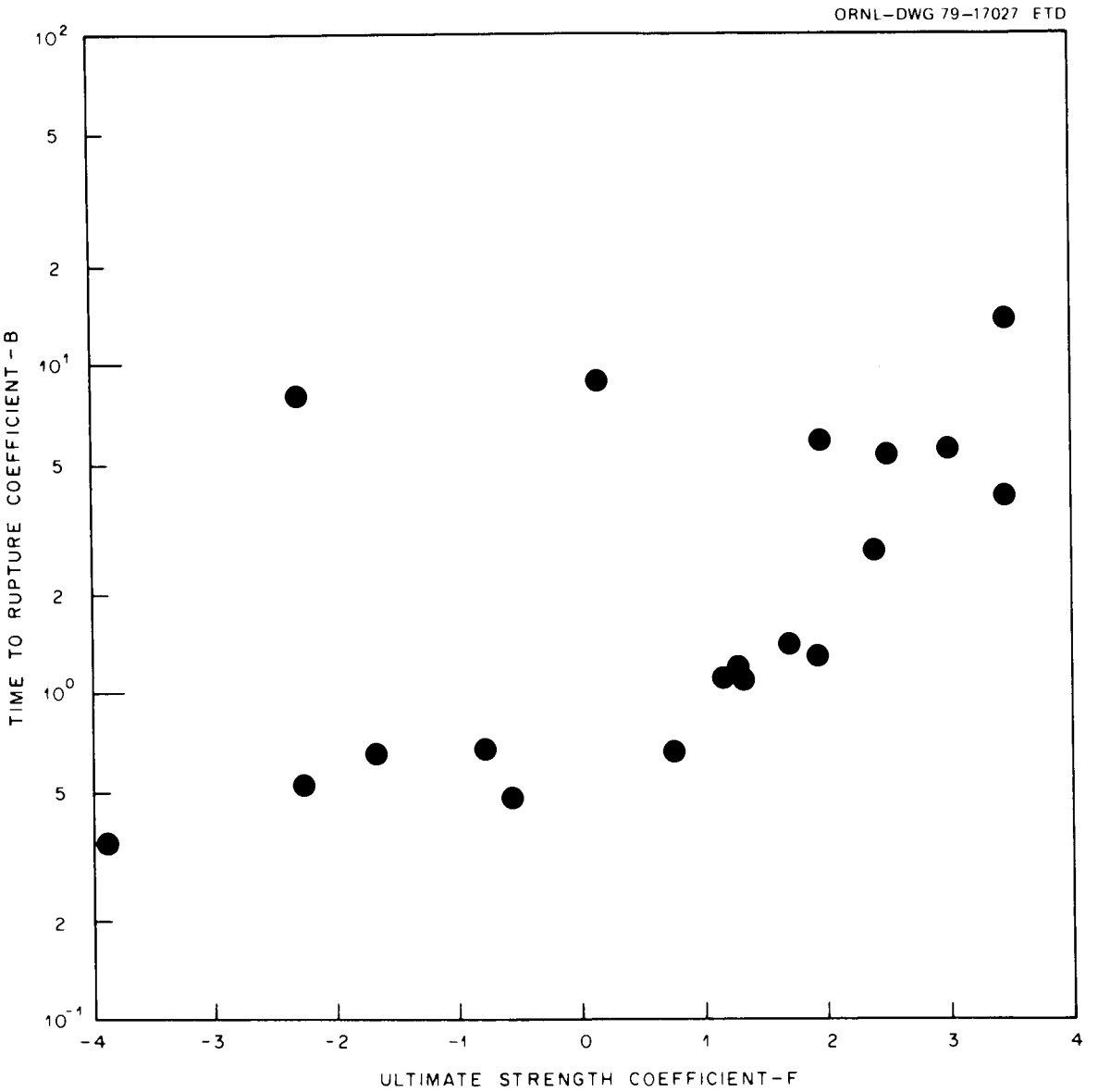

Fig. 26. Comparison of ultimate strength with time-to-rupture heat adjustment factors, F and B, for 19 heats of type 304 stainless steel.

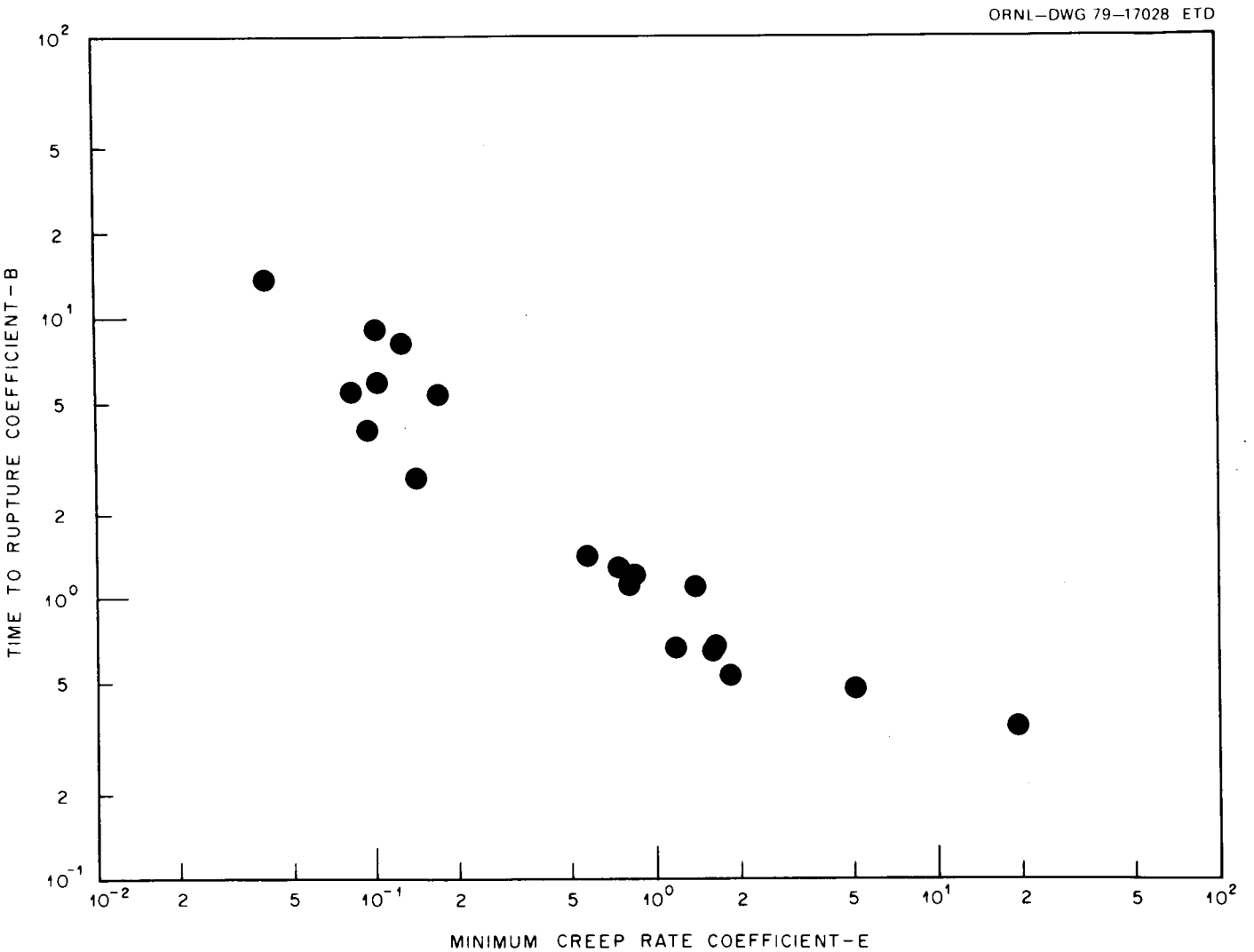

Fig. 27. Comparison of minimum creep rate with time-to-rupture heat adjustment factors, E and B, for 19 heats of type 304 stainless steel at 593°C (1100°F).

4. SUMMARY AND CONCLUSIONS

A study was performed to determine the heat-to-heat variability of mechanical properties used in performing inelastic analyses. The results are to be used to investigate the potential effects of material variability on conservation in ASME design margins.

Structural problems studied involved the ratchetting of a long thin-walled pipe. The load cycle consisted of a thermal down shock on the inner pipe wall from 593 to 427° C and a slow reheat followed by an isothermal hold under internal pressure at 593° C. The pipe response is a plastic cycle followed by isothermal creep.

To program the inelastic deformation and failure analysis of this problem, ten mechanical and physical material properties are needed. This study concentrated on what was considered the most important mechanical properties: monotonic and cyclic yield, plastic modulus, isothermal creep, stress rupture, and fatigue.

Data on 20 heats of type 304 stainless steel were compiled and analyzed. The intent was to develop simple heat-dependent parametric representations of each property. Cross correlations between properties were investigated also. Identified cross correlations could be used to reduce the number of inelastic analyses required and also to develop heat-dependent representations of properties where limited data exist. Analysis of the data indicated only one such strong cross correlation—between time-to-rupture and minimum creep rate.

Using the available data, heat-dependent correlations were developed for initial bilinear yield vs temperature, time-to-rupture vs stress at 593° C, and creep strain vs stress and time at 593° C. Cyclic yield stress was modeled based on an incremental increase in yield with accumulated plastic strain. The incremental yield stress vs plastic strain matrix was available for a single heat but was applied to all heats. Because yield for subsequent cycles was based on initial yield, cyclic yield had the same heat and temperature dependency as initial bilinear yield. Heat dependency of plastic modulus (or hardening parameter) vs temperature could not be demonstrated primarily due to lack of data. Use of a temperature- and heat-independent mean value of hardening parameter was thus recommended.

Time-to-rupture data at 593° C could be adequately correlated using a simple power law expression. Other parametric representations were examined, but the power law seemed best to model the data.

Creep deformation was represented using a three-term exponential equation with heat-dependent coefficients. These coefficients were calculated using the rational polynomial parameters C and p which are functions of minimum creep rate and time-to-rupture. Minimum creep rate was represented using a power law, and, for creep deformation only, time-to-rupture was expressed in terms of a cross correlation of minimum creep rate. This reduced the number of random variables needed to model heat-dependent creep deformation in the inelastic analyses. The resultant creep equation adequately represented the data.

Based on work at ANL[29] as well as on an assessment in this study, heat dependency of fatigue behavior was found to be very weak. Thus, the recommendation was made that fatigue damage be heat independent and that a fatigue failure correlation developed by Diercks and Raske[29] be used.

Results of this investigation appear to represent adequately the heat-to-heat variability of the mechanical properties studied. Some simplifications used in analyzing the data were shown to have surprisingly small effects on representing behavior for individual heats. This study was limited in that only certain mechanical properties were considered. The impact of variability in physical properties was not investigated. Attention should be given in future work to those mechanical and physical properties that were not considered in this study.

REFERENCES

1. U.S. Department of Energy, *Nuclear Systems Materials Handbook,* TID 26666, Hanford Engineering Development Laboratory, Richland, Wash.

2. ASME Code Case N-47-13, *Cases of ASME Boiler and Pressure Vessel Code,* American Society of Mechanical Engineers, New York, 1978.

3. W. K. Sartory and W. J. McAfee, *Materials Heat-to-Heat Variability Study: Part II—Analysis of the Effect on the Conservatism of Current Inelastic High-Temperature Structural Design Procedures,* ORNL-5605 (December 1980).

4. H. E. McCoy, *Tensile and Creep Properties of Several Heats of Type 304 Stainless Steel,* ORNL/TM-4709 (November 1974).

5. V. K. Sikka et al., *Tensile Properties of Type 304 Stainless Steel,* ORNL-5235 (February 1978).

6. *ASME Boiler and Pressure Vessel Code, Section III, Rules for Construction of Nuclear Power Plant Components,* 1977.

7. John Mandel and Robert C. Paule, "Interlaboratory Evaluation of a Material with Unequal Numbers of Replicates," *Anal. Chem.* **42**(11), 1194–1197 (September 1970).

8. Irwin Miller and John E. Freund, *Probability and Statistics for Engineers,* Prentice-Hall, Englewood Cliffs, N. J., 1965.

9. R. W. Swindeman et al., *Product Form Characterization of Type 304 Stainless Steel (Heat 9T2796),* ORNL-5222 (February 1977).

10. J. M. Steichen, *High Strain Rate Mechanical Properties of Types 304 and 316 Stainless Steel (RM-17),* HEDL-TME 71-164 (November 1971).

11. V. K. Sikka et al., *Influence of Laboratory Annealing on Tensile Properties of Time-Independent Design Stress Intensity Limits for Type 304 Stainless Steel,* ORNL-5175 (December 1976).

12. P. S. Maiya, *Bilinear Cyclic Stress-Strain Parameters for Type 304 and 316 Stainless Steel,* ANL-78-57 (July 1978).

13. J. M. Corum, M. Richardson, and J. A. Clinard, *Elevated-Temperature Benchmark Tests of Simply Supported Beams and Circular Plates Subjected to Time-Varying Loadings,* ORNL-5301 (September 1977).

14. C. F. Cheng and C. Y. Cheng, *Bilinear Representations of the Cyclic Stress-Strain Behavior of Types 304 and 316 Stainless Steel from 800 to 1200°* F, ANL-8002 (February 1974).

15. C. F. Cheng and C. Y. Cheng, *Bilinear Representations of Stress-Strain Behavior of Types 304 and 316 Stainless Steel Cyclically Deformed at 800 to 1200° F,* Paper L 3/7, Second International Conference on Structural Mechanics in Reactor Technology, Berlin, Federal Republic of Germany (September 1973).

16. Private communication, V. K. Sikka to W. J. McAfee, Letter. No. 0517-28-79, May 17, 1979.

17. U.S. Energy Research and Development Administration, *Guidelines and Procedures for Design of Nuclear Systems Components at Elevated Temperatures,* RDT Standard F9-5T (March 1974).

18. J. M. Corum, "Appendix: Material Property Data for Elastic-Plastic-Creep Analysis of Benchmark Problems," pp. 99–109 in *Pressure Vessels and Piping: Verification and Qualification of Inelastic Analysis Computer Programs,* ASME Publication G00088 (1975).

19. M. K. Booker, *Mathematical Analysis of the Elevated-Temperature Creep Behavior of Type 304 Stainless Steel,* ORNL/TM-6110 (December 1977).

20. V. K. Sikka, M. K. Booker, and C. R. Brinkman, *Use of Ultimate Tensile Strength to Correlate and Estimate Creep and Creep-Rupture Behavior of Types 304 and 316 Stainless Steel,* ORNL-5285 (October 1977).

21. R. W. Swindeman, "Creep Correlation for Type 304 Stainless Steel (Heat 9T2796)," pp. 1—30 in *Structural Materials for Service at Elevated Temperatures in Nuclear Power Generation, ASME, MPC-1,* Symposium held Nov. 30—Dec. 3, 1975, Houston, Tex.

22. C. E. Pugh, "Creep Law Development for the ORNL Reference Heat of Type 304 Stainless Steel at 1100°F," pp. 31–43 in *High-Temperature Structural Design Methods for LMFBR Components Quarterly Progress Report for Period Ending September 30, 1972,* ORNL/TM-4058 (January 1973).

23. W. E. Leyda and C. C. Schultz, *Variability in Creep and Rupture Test Results in a Single Heat of Type 304 Stainless Steel,* ORNL/Sub-3654-3, Babcock & Wilcox Company (September 1975).

24. L. D. Blackburn, "Isochronous Stress-Strain Curves for Austenitic Stainless Steels," pp. 15–48 in *The Generation of Isochronous Stress-Strain Curves,* American Society of Mechanical Engineers Publication for Winter Annual Meeting, Nov. 26–30, 1972.

25. M. K. Booker and V. K. Sikka, *Analysis of the Creep Strain-Time Behavior of Type 304 Stainless Steel,* ORNL-5190 (October 1976).

26. W. K. Sartory, *PLACRE Users Manual,* ORNL/TM-5626 (February 1977).

27. J. M. Corum et al., *Thermal Ratchetting Tests of Type 304 Stainless Steel Pipe: Specimen TTT-1 and TTT-2,* ORNL-5386 (June 1978).

28. J. A. Clinard, "International Piping Benchmark Effort, Creep Equation," pp. 137–140 in *High Temperature Structural Design Program Semiannual Progress Report for Period Ending June 30, 1978,* ORNL-5433 (November 1978).

29. D. R. Diercks and D. T. Raske, *Elevated-Temperature, Strain-Controlled Fatigue Data on Type 304 Stainless Steel: Compilation, Multiple Linear Regression Model, and Statistical Analysis,* ANL-76-95 (December 1976).

ACKNOWLEDGMENT

The authors wish to thank J. M. Corum who suggested this study and J. A. Clinard and M. K. Booker who reviewed the manuscript.

ORNL-5604
Dist. Category UC-79, -79h, -79k

Internal Distribution

1. R. L. Battiste
2. J. J. Blass
3. S. E. Bolt
4. M. K. Booker
5. C. R. Brinkman
6. J. W. Bryson
7. J. A. Clinard
8. J. M. Corum
9. J. R. Ellis
10. W. L. Greenstreet
11. R. C. Gwaltney
12. W. O. Harms
13. R. L. Huddleston
14. S. K. Iskander

15–19. W. J. McAffee

20. H. C. McCurdy
21. J. G. Merkle
22. E. T. Onat (consultant)
23. P. Patriarca
24. C. E. Pugh
25. J. L. Rich
26. M. Richardson
27. D. N. Robinson

28–32. W. K. Sartory

33. J. E. Smith
34. R. W. Swindeman
35. H. E. Trammell
36. G. D. Whitman
37. G. T. Yahr
38. Patent Office
39. Central Research Library
40. Document Reference Section

41–42. Laboratory Records Department

43. Laboratory Records (RC)

Subcontractors

44. H. Armen, Jr., Grumman Aerospace Corp., Bethpage, NY 11714
45. C. E. Jaske, Battelle-Columbus Laboratories, Columbus, OH 43201
46. W. J. O'Donnell, O'Donnell and Associates, Pittsburgh, PA 15232
47. D. H. Pai, Foster-Wheeler Energy Corp., Livingston, NJ 07029
48. C. C. Schultz, Babcock and Wilcox Co., P. O. Box 835, Alliance, OH 44601

External Distribution

49–50. Director, Office of Reactor Research and Technology, Department of Energy, Washington, DC 20545

51. Office of Assistant Manager for Energy Reserach and Development, DOE, ORO, Oak Ridge, TN 37830
52. Director, Nuclear Research and Development Division, DOE, ORO, Oak Ridge, TN 37830

53–234. Given distribution as shown in DOE/TIC-4500 under categoreis UC-79, -79h, -79k